Gondwana Research 156 (2026) 354–371

Contents lists available at ScienceDirect

Gondwana Research

journal homepage: www.elsevier.com/locate/gr

Research Paper

Age and provenance constraints for the geodynamic evolution of the Indus Suture Zone during the Cenozoic

Lucas Vimpere [a,*], Pierre Bouilhol [b], Pietro Sternai [c], Speranta-Maria Popescu [d], Jean-Pierre Suc [d,e], Spela Gorican [f], Marc Poujol [g], Nathan Cogné [g], Germain Bayon [h], Anne Trinquier [h], Thierry Adatte [i], Jorge E. Spangenberg [j], Marcel Regelous [k], Christian Vérard [a], Rajeev Upadhyay [l], Sébastien Castelltort [a]

[a] Department of Earth Sciences, University of Geneva, Rue des Maraîchers 13, 1205 Geneva, Switzerland
[b] Université de Lorraine, CNRS, CRPG, Nancy, France
[c] Earth and Environmental Sciences (DISAT), University of Milano-Bicocca, Viale Piero e Alberto Pirelli, 7106/Edificio U4, 20126 Milan, Italy
[d] GeoBioStratData.Consulting, 385 Route du Mas Rillier, 69140 Rillieux-la-Pape, France
[e] Sorbonne Université, CNRS-INSU, Institut des Sciences de la Terre Paris, UMR, 75005 Paris, France
[f] Ivan Rakovec Institute of Paleontology, Research Centre of the Slovenian Academy of Sciences and Arts (ZRC SAZU), Novi trg 2, 1000 Ljubljana, Slovenia
[g] Université de Rennes, CNRS, Géosciences Rennes, UMR 6118, F-35000 Rennes, France
[h] Institut Français de Recherche pour l'Exploitation de la Mer (IFREMER), Centre Bretagne - ZI de la Pointe du Diable - CS 10070, 29280 Plouzané, France
[i] Institute of Earth Sciences (ISTE), University of Lausanne, Géopolis, 1015 Lausanne, Switzerland
[j] Institute of Earth Surface Dynamics (IDYST), University of Lausanne, Géopolis, 1015 Lausanne, Switzerland
[k] GeoZentrum Nordbayern, University of Erlangen-Nürnberg, Schlossgarten 5, 91054 Erlangen, Germany
[l] Geology Department, Kumaun University, Sleepy Hollow, Nainital 263001 Uttarakhand, India

ARTICLE INFO

Keywords:
India collision
Ladakh
Foreland basin
Indus molasse
Palynology

ABSTRACT

The timing of the India-Asia collision and the multi-stage tectonic control on the development of Himalayan sedimentary basins has remained controversial for over half a century. In particular, it remains unclear whether the stratigraphic record of the Indus Suture Zone (ISZ) in Ladakh, NW India, 1) preserves pre-collisional trench deposits, 2) whether the cessation of marine sedimentation reliably marks continental collision, and 3) how provenance and depositional ages inform on the geodynamic evolution of the orogeny.

This study re-examines the tectonostratigraphic evolution of the Indus Basin in the region by leveraging new biostratigraphic data (radiolarians, dinoflagellates) and detrital zircon U-Pb ages. We further integrate whole-rock and clay-size fraction geochemical and Nd isotopic data to constrain provenance changes and their relationship to major tectonic events pertaining to the collision between India and the Kohistan-Ladakh intra-oceanic arc (KLA).

Results show that the stratigraphic record in the region exclusively preserves the Paleogene-Neogene syn- to post-collisional foreland sedimentation (< ca. 54 Ma). Deposition, sediment supply, and drainage patterns were largely controlled by 1) the Spongtang ophiolite obduction (64–42 Ma) onto the Indian margin, 2) the collision-induced uplift of the KLA (53–40 Ma), and 3) the exhumation of the Tso Morari complex (45 Ma). Importantly, the diachronous cessation of plain marine conditions between the northern (50 Ma) and southern (40 Ma) margins of the Eocene foredeep warns against relying on the last occurrence of marine units as a uniquevocal marker for continental collision onset. Instead, the oldest foreland deposits only provide a minimum age constraint (ca. 54 Ma) for the India-KLA collision.

These results highlight the relevance of applying a multi-proxy approach for reconstructing the evolution of collisional orogens. Furthermore, we demonstrate that palynological analyses in the Himalayas and adjacent basins constitute an effective dating method to accurately time tectonostratigraphic events.

* Corresponding author.
E-mail address: Lucas.Vimpere@unige.ch (L. Vimpere).

https://doi.org/10.1016/j.gr.2026.03.014
Received 11 July 2025; Received in revised form 23 March 2026; Accepted 24 March 2026
Available online 25 April 2026

1. Introduction

The Himalayan orogeny ranks amongst the most extensively studied tectonic events and results from the closing of the Tethys and the ensuing continental collision between the Indian and Eurasian plates. However, the nature of the collision and kinematic evolution of the system remain contentious to this day. Although most models for Neo-Tethys closure assumed a single-stage collision with an Andean-type subduction zone beneath Asia, the geological record of convergence attest for an intra-oceanic subduction zone that separated the Indian plate to the south from the Eurasian continental block to the north (e.g., Aitchison et al., 2000; Andjić et al., 2022; Bouilhol et al., 2013; Reynolds et al., 1983; Searle et al., 1987). The NW Himalaya is of particular interest as it preserved the Kohistan-Ladakh intra-oceanic island arc (KLA; Fig. 1), which constitutes evidence of the equatorial Trans-Tethyan subduction (Martin et al., 2020), holding clues to collisional dynamics (e.g., Burg and Bouilhol, 2019; Garzanti et al., 1987; Honegger et al., 1982; Zhang et al., 2023).

The Ladakh region is of particular importance for defining the Indus Suture Zone (ISZ), which marks the India-KLA collision, here defined as the moment when the Neo-Tethys oceanic lithosphere was fully subducted (Beck et al., 1995). The cessation of marine sedimentation as preserved in the ISZ stratigraphic record has been used to elaborate on the timing of the Neo-Tethys closure and subsequent continental collision (e.g., Henderson et al., 2011; Hu et al., 2016; Rowley, 1996). However, the accurate dating of sedimentary formations has long been hampered by scarce microfauna and flora, presumably due to substantial sedimentation rates in the basin. The introduction of detrital zircon (DZ) U-Pb dating has provided numerous ages since then, but their reliability to accurately date sediment deposition has been questioned (e.g., Sharman and Malkowski, 2020). Building up on previous work, we here propose a revised stratigraphy and evolutional history of the Indus Basin in Ladakh based on new sedimentary, geochemical, and geochronological data. We also present the first extensive palynological dataset for the region, bringing new insights on the provenance, age, and depositional environment of the exposed units. Ultimately, this study discusses the relevance of using the regional stratigraphic record to date the India-KLA collision.

1.1. Geological setting

From the south to the north, six major tectonic zones have been recognised in the ISZ (Fig. 1). The **Tethyan Himalayan Sequence** consists of the Late Triassic to Early Eocene sedimentary cover of the Greater India passive margin. It consists of the Zanskar Gp shelf limestones (Garzanti et al., 1987; Green et al., 2008; Mathur et al., 2009) and the coeval distal-slope flysch of the Lamayuru Fm (Brookfield and Andrews-Speed, 1984; Frank et al., 1977; Fuchs and Linner, 1995; Honegger et al., 1982).

The **Indus Suture Zone (ISZ)** marks the India-KLA collisional

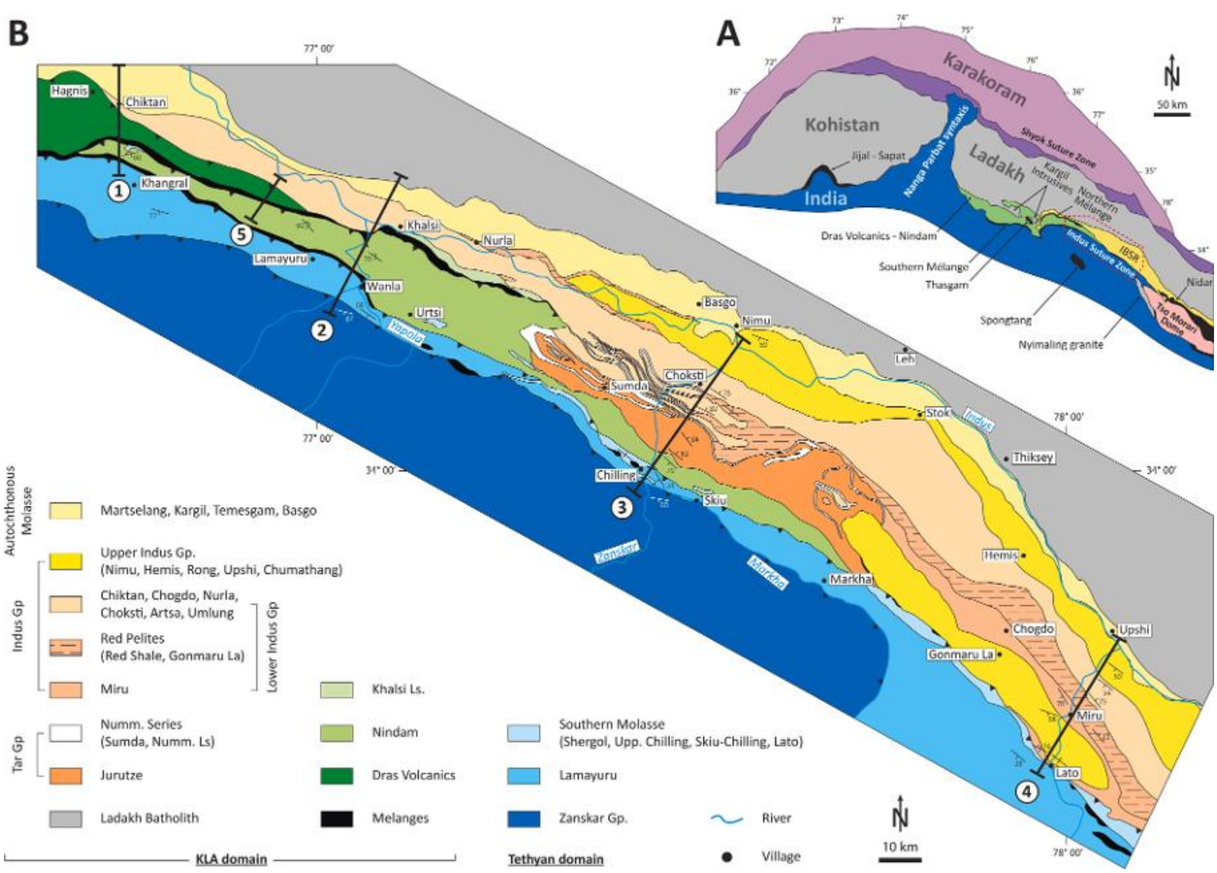

Fig. 1. A: Simplified geological map of the NW Himalaya showing the location of B (red dotted polygon) and the main units discussed in the text (map modified from Bouilhol et al., 2013; Buchs, 2019; Martin et al., 2025b; Robertson and Degnan, 1994; Robertson, 2000; Rolland et al., 2002; Steck, 2003). B: Geological map of Ladakh showing the major structural units preserved as nappes within the Indus Suture Zone, between the paleo-Indian continental passive margin (Tethyan domain) to the south and the Ladakh Batholith to the north. The formations and lateral correlations are based on ground-truth observations collected for this study and combined with previous work (Brookfield and Andrews-Speed, 1984; Clift et al., 2002a, 2002b, 2001, 2000; Corfield and Searle, 2000; Fuchs, 1986, 1984, 1979, 1977; Fuchs and Linner, 1995; Gupta and Kumar, 1975; Henderson et al., 2011, 2010; Searle et al., 1990; Steck, 2003; Sutre, 1990; Van Haver, 1984). Studied and samples sections are as follows. 1: Chiktan valley; 2: Yapola gorge; 3: Zanskar gorge; 4: Upshi-Lato; 5: Takmachik valley. (For interpretation of the references to colour in this figure legend, the reader is referred to the web version of this article.)

boundary and is wedged between the Tethyan Himalayan sequence and the ***Kohistan-Ladakh Arc (KLA)***. It hosts the pre- and post-collisional units ranging from the Jurassic to Miocene in age, that were subsequently subject to fold-thrust deformation. The oldest outcropping units are the ***Northern and Southern Mélanges***, which result from a complex series of multi-stage tectonic processes, involving subduction, ophiolite emplacement, syn- and post-collisional events (Robertson, 2000). Amongst other components (e.g., serpentinite, basalts, blueschists), they comprise blocks of radiolarian cherts from the Jurassic to Late Cretaceous (Honegger et al., 1982; Sutre, 1990). More recently, geochemical analyses evidence the ***Spongtang Ophiolite*** as the main source of the detrital chrome spinels contained in the Southern Mélange in the Zanskar gorge (Baxter et al., 2016). The authors thus concluded that its final emplacement must have occurred after the obduction of the Spongtang Ophiolite onto the Indian plate (ca. 55–50 Ma), later supported by *in-situ* radiometric dating (between 64.3 ± 0.8 and 42.4 ± 0.5 Ma; Catlos et al., 2019).

In western Ladakh, the Mélanges bound the ***Nindam Fm***, interpreted as the erosion product (Van Haver, 1984) of the Cretaceous ***Dras Volcanics*** (Reuber, 1989) and ***Kargil Intrusives*** (Honegger et al., 1982). The Nindam Fm succession starts with deep-water volcaniclastic turbidites accumulating as a distal forearc apron (Robertson and Degnan, 1994) and passes upwards into shallow marine system deposits (Searle et al., 1990). Palynological evidence and DZ U-Pb ages point towards a deposition of the Nindam Fm from the Early Cretaceous to Late Paleocene (Upadhyay et al., 2004; Walsh et al., 2019). In eastern Ladakh, the Southern Mélange is unconformably overlain by the oldest units of the Indus Basin Sedimentary Rocks (IBSR), namely the Early Eocene marine sequence of the ***Tar Gp*** shallowing upwards (Henderson et al., 2010; Searle et al., 1990; Sinclair and Jaffey, 2001). For some authors, the upper boundary the Tar Gp marks the cessation of plain marine conditions in the basin and thus, pinpoints the final closure of the Neo-Tethys and subsequent continent–continent collision (50 Ma; Garzanti et al., 1987; Henderson et al., 2011, 2010; Rowley, 1996; Searle et al., 1987; Van Haver, 1984). The Tar Gp is unconformably overlain by younger sedimentary units marking the transition towards a continental molasse within the foreland basin (Henderson et al., 2010; Searle et al., 1990; Sinclair and Jaffey, 2001).

Based on their provenance, three types of molasses have been described in the region. The ***Indus Gp*** molasse shows an evolution from Middle Eocene fluvio-deltaic facies to more proximal alluvial facies deposited from Late Eocene to Late Oligocene (Bhattacharya et al., 2021; Henderson et al., 2010; Wu et al., 2007). From west to east, it lies in unconformable contact above the Dras Volcanics in the Chiktan valley (Chiktan Fm), Northern Mélange in the Yapola gorge (Chiktan Fm), and Tar Gp in the Zanskar gorge (Chogdo, Choksti, and Nimu Fms). Further east along the Upshi-Lato section, the Indus Gp is fault-bound against the India-derived coarse conglomerates of the ***Southern Molasse*** (i.e., Lato and Upper Chilling Fms of (Henderson et al., 2011, 2010), which was tentatively dated at the Lato village by DZ U-Pb at 51.1 ± 0.7 Ma (Henderson et al., 2011). The Southern Molasse is locally overlying the Southern Mélange (e.g., Zanskar gorge), Nindam Fm (e.g., Markha valley), and Lamayuru Fm (e.g., Lato village; Brookfield and Andrews-Speed, 1984; Clift et al., 2002a, 2001; Fuchs and Linner, 1995; Henderson et al., 2011; Sterne, 1979; Sutre, 1990; Van Haver, 1984). Finally, the KLA is unconformably overlain by the Late Oligocene to Miocene ***Autochthonous Molasse*** (Bhattacharya et al., 2021; Zhou et al., 2020).

To the east, the whole sedimentary basin is structurally perturbed by the presence of the Tetraogal nappe stack and associated **Tso Morari Complex** (Long et al., 2020), which represents the metamorphosed (UHP and Barrovian) Indian continental margin. The complex is characterised by Ordovician granites intruding Precambrian-Cambrian sediments, which underwent ultra-high-pressure metamorphism during the subduction of India beneath Eurasia (50.8 ± 1.4 Ma), before being exhumated (45–30 Ma; St-Onge et al., 2013). The Tso Morari dome is bounded to the north by the **Nidar Ophiolite** (Thakur and Virdi, 1979), a suprasubduction-zone ophiolitic sequence (Mahéo et al., 2004) that records early-stages of intra-oceanic subduction within the Neo-Tethys (140 ± 32 Ma; Ahmad et al., 2008).

The **KLA** built up within the Neo-Tethys (Martin et al., 2020) onto the oceanic basement (Villalobos-Orchard et al., 2025) between the Middle Jurassic and the Late Eocene (Bouilhol et al., 2013; Jagoutz et al., 2019). It comprises the arc granitic ***Kohistan-Ladakh Batholith*** (***KLB***) and its volcanic cover, which is mainly represented in Ladakh by: the Dras (165–80 Ma; Walsh et al., 2021), Teah (Raz and Honegger, 1989; zircon U-Pb: 62.9 ± 0.4 Ma; Supp. Data Table S1-S3), Deosai (123–46 Ma; Jadoon et al., 2020), and Khardung Volcanics (69–52 Ma; Bhutani et al., 2009; Singh et al., 2023). Part of the arc basement is now thrusted upon the Tethyan Sequence such as the Spongtang Ophiolite (Catlos et al., 2019; Reuber, 1986).

To the north, the **Shyok Suture Zone** separates the KLA from the **Karakoram Batholith**, the Andean type, Eurasian continental margin, whose geodynamic history is beyond the scope of this paper (Bouilhol et al., 2013; Martin et al., 2025a).

2. Methods

Investigations were carried along five main cross sections: the Chiktan valley, Yapola and Zanskar gorges, and Upshi-Lato section (Figs. 1 and 2), with additional sampling in the Takmachik valley. Biostratigraphic ages of the units are based on radiolarian and dinoflagellates assemblages (Supp. Data Textt, Table S1 and S2). Radiometric ages were determined through zircon U-Pb geochronology using laser ablation mass spectrometry. The DZ U-Pb ages of sedimentary units reported in this study (Table 1) use the youngest single grain (YSG) measures as maximum depositional ages (MDAs); the rationale for this approach is detailed in the Supp. Data Text. Provenance was investigated by combining DZ U-Pb age populations, as well as whole-rock and clay geochemistry, and Nd isotopic composition on clay-size fractions. Refer to Supp. Data for details on sample locations, analytical procedures, data treatment, detailed results.

3. Depositional timing of the IBSR

3.1. Southern Mélange and Dras Volcanics

Two radiolarian cherts (n = 2) within the Southern Mélange are Early Cretaceous (Berriasian-Valanginian, 145–132.6 Ma) in age in the Chiktan valley, and Early Jurassic (Pliensbachian, 192.9–184.2 Ma; Figs. 3-4; Supp. Data Text) in the Yapola gorge, similar to the ones reported for laterally-equivalent sections in Ladakh and Pakistan (Robertson, 2000). Two U-Pb ages were obtained on zircon grains from two samples (n = 2) of the Dras Volcanics (Table 1; Figs. 3-4), one Concordia age (157.94 ± 0.70 Ma) from an andesitic lava flow deposit and one YSG age (166.2 ± 4.0 Ma) from a volcaniclastic sandstone, supporting previous estimates (Walsh et al., 2021) and overall confirming the Jurassic arc inception (Jagoutz et al., 2019).

3.2. Tar Gp

The sediments of the Tar Gp and are mostly exposed in the Zanskar gorge, where they are heavily folded (Brookfield and Andrews-Speed, 1984). As all six samples we analysed for palynological dating proved to be barren, this study relies on age constraints provided by previous investigations. The Tar Gp forms a shallowing-upward marine sequence that is subdivided into three formations. The basal shallow sandy turbidites of the Jurutze Fm (55.1 ± 1.3 Ma, Andjić et al. 2022; 53.4 ± 1.4 Ma, Henderson et al., 2010) evolve towards more frequent calciturbidites and discrete carbonate levels of the Sumda Fm (54.9–51 Ma; Henderson et al., 2010), culminating in the uppermost shallow platform carbonates of the Nummulitic Limestone Fm (Numm. Ls.; 50.8–49.4 Ma;

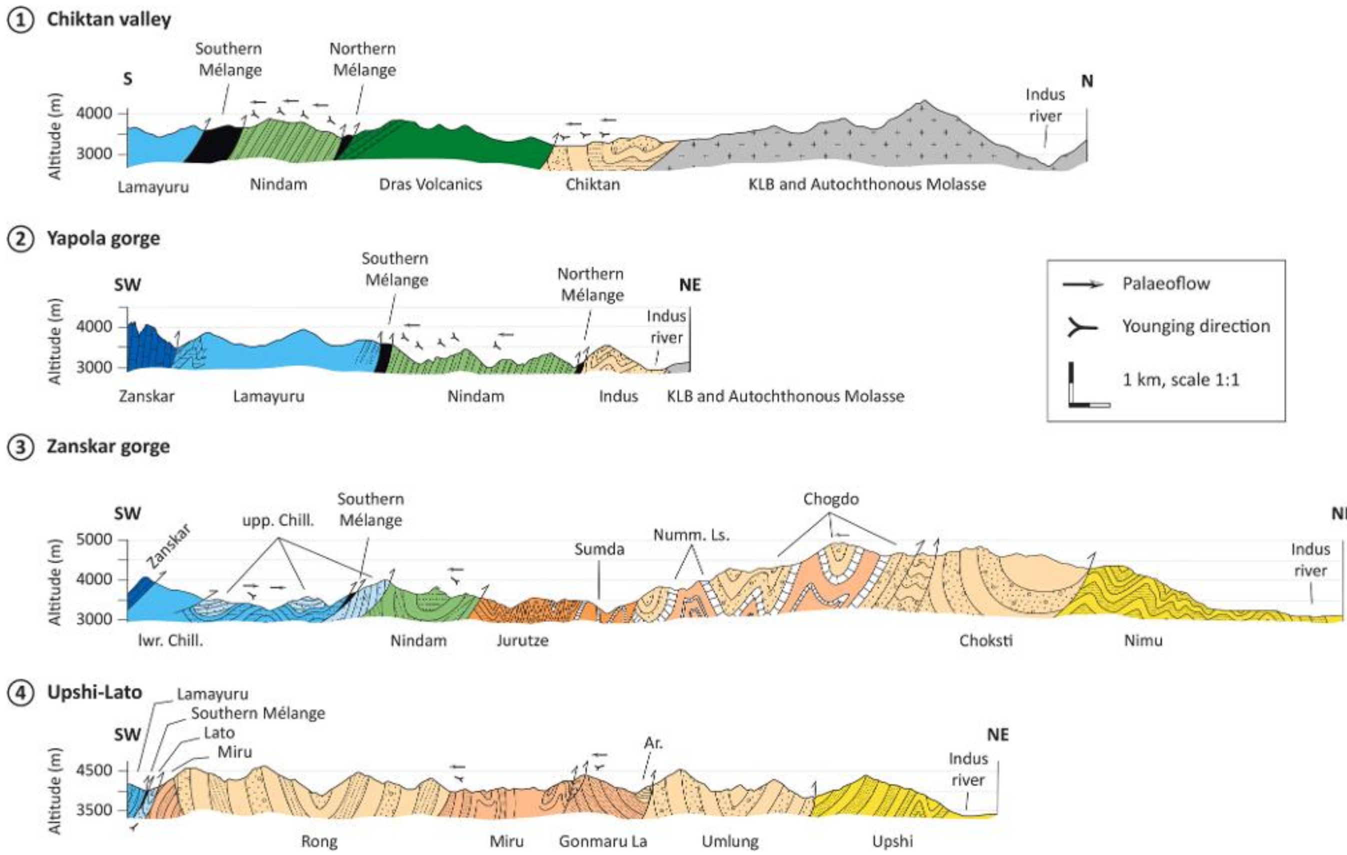

Fig. 2. Cross-sections illustrating the stratigraphic and structural relationships between the formations of the Indus Basin along the studied transects. Numbers correspond to the section locations in Fig. 1.

Henderson et al., 2010).

3.3. Lwr. Indus Gp and Nindam Fm

Continental sedimentation in the ISZ is first featured by the lwr. Indus Gp molasse, which overlies the Tar Gp and was deposited in continental (i.e., alluvial, palustrine, meandering fluvial) and inner neritic (i.e., coastal, lagoonal, deltaic) environments (Supp. Data Table S2; e.g., Garzanti and Van Haver, 1988; Henderson et al., 2010; Searle et al., 1990; Zhou et al., 2020). In the Zanskar gorge, the basal lwr. Indus Gp comprises the Chogdo Fm (n = 2) and Nurla Fm (n = 1), dated by DZ U-Pb at 49.8 ± 1.2 and 50.4 ± 2.1 Ma, respectively (Table 1; Fig. 4). Conglomeratic levels are found discordant over the Sumda Fm and contain reworked carbonate clasts from the Numm. Series of the underlying Tar Gp. If considered autoclastic, the Chogdo Fm is at most contemporaneous to the Numm. Ls. (Henderson et al., 2010). Consequently, and based on their similar facies (Clift et al., 2002a; Henderson et al., 2010), we consider the Chogdo and Nurla Fms to be one tectonostratigraphic unit and will hereafter simply refer to it as the Chogdo Fm. It is unconformably overlain by the Choksti Fm, from which it is separated by the Choksti thrust (Sinclair and Jaffey, 2001). Only one out of three samples returned a biostratigraphic age at 47.3–21 Ma (Fig. 4), which agrees with published DZ U-Pb ages (45.5 Ma; Henderson et al., 2010; Wu et al., 2007). The biostratigraphic extension of the Choksti Fm up to the Miocene is supported by the Late Eocene (< 23.7 ± 0.2 Ma) to Late Miocene (< 6.11 ± 2.3 Ma) ^{40}Ar-^{39}Ar ages (Fig. 4) retrieved from youngest white micas in the lower and upper levels of the overlying Nimu Fm by Henderson et al. (2011, 2010).

Further east in the Upshi-Lato section, the deltaic Miru Fm (Henderson et al., 2011) is fault-bound to the north by the lacustrine red shales of the Gonmaru La Fm (Fuchs and Linner, 1995; Garzanti and Van Haver, 1988; Henderson et al., 2011). DZ U-Pb ages (Table 1; Fig. 4) argue for the Gonmaru La Fm (n = 1; 51.3 ± 1.5 Ma) being older than the Miru Fm (n = 5; 43.4 ± 4.7 Ma). In contrast, overlapping biostratigraphic ages from the Gonmaru La Fm (n = 2; 47.3–21 Ma) and Miru Fm (n = 4; 40.6–32.3 Ma) suggest that these units are contemporaneous (Fig. 4). Both are tentatively attributed to the lwr. Indus Gp based on similar facies and stratigraphic position within the basin (Henderson et al., 2010), although more data are required to validate this correlation. Late Eocene to Late Oligocene ^{40}Ar-^{39}Ar ages from youngest white micas in the overlying Upshi Fm (Henderson et al., 2011) broadly agree with the biostratigraphic extensions determined for the Gonmaru La Fm.

In western Ladakh, the Dras Volcanics are overlain by the fluvio-alluvial Chiktan Fm to the north and by the turbiditic Nindam Fm. to the south. The Chiktan Fm. yielded concordant biostratigraphic (n = 2; 40.4–32.3 Ma) and DZ U-Pb (n = 1; 41.6 ± 1.0 Ma) ages (Table 1; Fig. 4). Contemporaneous biostratigraphic ages were retrieved from the Nindam Fm. (n = 12; 40.6–32.3 Ma; Fig. 4), which corroborate the Paleocene palynological assemblages described by Upadhyay et al. (2004). These data contrast with the obtained Late Cretaceous DZ U-Pb ages (n = 7; 69.1 ± 5.6 Ma; Table 1; Fig. 4) and previous interpretations (Andjić et al., 2022; Clift et al., 2002b; Van Haver, 1984; Walsh et al., 2019), which mostly reflects inherited zircons from the Dras Volcanics and Kargil Intrusives sourcing the Nindam Fm. This discrepancy is further discussed in more details in *section 4*.

3.4. Upp. Indus Gp

The upp. Indus Gp displays conglomeratic facies showing a general coarsening-up trend towards younger formations (Henderson et al., 2010; Sinclair and Jaffey, 2001). It was deposited in a more proximal

Table 1

Summary of U-Pb ages ($^{206}Pb/^{238}U$) of magmatic (in bold) and detrital zircons. Magmatic zircon ages are reported as Concordia ages, whereas detrital zircon ages are reported using the youngest single grain (YSG), the YSG Concordia (YSG_c), and youngest cluster ages calculated from two or more overlapping grains within 1σ (YC1) and 2σ (YC2) uncertainty. All ages reported in the main text are using YSG ages as maximum depositional ages (MDAs); the rationale for this approach is detailed in the Supp. Data Text. Unit names previously used by other authors (e.g. Henderson et al., 2010) and now grouped under the Chogdo Fm in this study are marked with an asterisk.

# Sample	Lat.	Long.	Section	Lithology	Nbr. of grains	Nbr. of Concordia grains (−5 < dc < 10)	Concordia (Ma)	2S	YSG (Ma)	2S	YSGc (−5 < dc < 10)(Ma)	2S	YC1 (Ma)	2S	YC2 (Ma)	2S
Tethyan Domain																
Lamayuru																
LD22-06	34.03118	77.19384	Zanskar gorge	Conglomerate	38	31			45.6	1.5	45.6	1.5	86.1	1.3	85.8	1.2
Southern Molasse																
LD22-80	34.45263	76.52363	Chiktan valley	Conglomerate	110	92			41.5	1.1	41.5	1.1	44.2	0.9	42.7	0.8
LD22-126	33.68163	77.72526	Upshi-Lato	Sandstone	120	87			45.2	1.0	54.4	1.8	57.4	1.5	56.1	1.2
LD22-128	33.68163	77.72526	Upshi-Lato	Conglomerate carbonated	120	90			52.6	1.9	52.6	1.9	56.7	1.5	57.5	1.2
LD22-54	33.68187	77.72842	Upshi-Lato	Sandstone	118	92			56.9	1.5	77.2	2.7	450.8	3.1	450.8	3.1
LD22-10	34.04574	77.21220	Zanskar gorge	Conglomerate red	24	17			82.1	1.9	97.2	1.7	97.5	1.1		
KLA Domain																
Teah Volcanics																
LD19-68	34.35039	76.96963	Teah valley	Basaltic lava flow	30		**62.9**	**0.4**								
Dras Volcanics																
LD22-75	34.44105	76.52659	Chiktan valley	Andesite	30		**157.9**	**0.7**								
LD22-77	34.44105	76.52659	Chiktan valley	Andesite	2				166.2	4.0						
Nindam																
LD22-67	34.40174	76.52446	Chiktan valley	Sandstone	105	80			69.1	5.6	96.2	3.8	98.3	0.7	100.3	0.4
LD22-96	34.31902	76.83902	Yapola gorge	Sandstone carbonated	23	17			78.9	4.3	80.0	2.6	85.0	1.4	86.7	1.0
LD22-116	34.36011	76.73006	Takmachik valley	Sandstone	34	31			84.9	3.0	84.9	3.0	86.7	1.5	88.6	0.7
LD22-121	34.36476	76.73981	Takmachik valley	Sandstone	6	6			86.3	3.5	86.3	3.5	88.2	1.7	89.1	1.3
LD22-102	34.29274	76.81582	Yapola gorge	Sandstone	117	98			90.6	2.1	90.6	2.1	90.9	1.5	93.4	0.6
LD22-104	34.28536	76.81450	Yapola gorge	Sandstone	11	6			98.0	2.0	98.0	2.0	98.3	1.9	99.4	1.6
LD22-100	34.28879	76.79538	Yapola gorge	Sandstone	3	3			100.0	2.1	100.0	2.1				
Lwr. Indus Gp																
Chogdo																
LD22-24 (Chogdo*)	34.10736	77.21479	Zanskar gorge	Conglomerate green	68	55			49.8	1.2	49.8	2.2	49.8	1.0	51.3	0.8
LD22-35 (Nurla*)	34.12650	77.27107	Zanskar gorge	Sandstone green	127	118			50.4	2.1	50.4	2.1	50.9	1.1	51.2	1.0
LD22-33 (Chogdo*)	34.12916	77.24152	Zanskar gorge	Sandstone green	113	85			56.1	2.6	56.1	2.6	57.4	1.0	58.9	0.6
Chiktan																
LD22-84	34.46642	76.51446	Chiktan valley	Sandstone micaceous	47	31			41.6	1.0	45.7	0.7	46.0	0.5	46.5	0.3
Miru																
LD22-46	33.74135	77.75211	Upshi-Lato	Sandstone	120	106			43.4	4.7	50.2	2.5	50.1	1.6	52.6	0.6
LD22-50	33.74279	77.74708	Upshi-Lato	Sandstone	120	110			44.2	1.7	44.2	1.7	54.9	1.0	54.9	1.0
LD22-52	33.68171	77.72803	Upshi-Lato	Sandstone	77	51			46.9	1.4	46.9	1.4	52.7	1.3	54.0	0.7
LD22-61	33.74413	77.74323	Upshi-Lato	Sandstone	119	97			52.1	1.8	52.1	1.8	53.0	0.8	53.0	0.8
LD22-43	33.74509	77.75601	Upshi-Lato	Siltstone	2	2			76.0	1.7	76.0	1.7				
Gonmaru La																
LD22-62	33.74780	77.75855	Upshi-Lato	Sandstone fine	114	83			51.3	1.5	51.3	1.5	53.5	0.8	53.0	0.7
Upp. Indus Gp																
Rong																
LD22-60	33.74500	77.73803	Upshi-Lato	Sandstone	120	100			41.3	0.7	51.9	1.4	52.6	0.6	53.4	0.3
LD22-53	33.68187	77.72842	Upshi-Lato	Sandstone	120	95			48.1	1.3	48.1	1.3	48.8	0.5	48.8	0.5

(caption on next page)

Fig. 3. A: Early Cretaceous radiolarian chert bloc (Berriasian-Valanginian, 145–132.6 Ma) lying within a serpentinite-rich sandstone matrix (Chiktan valley; 34.39658°N, 76.52464°E; view to the NE). B: Early Jurassic radiolarian chert (Pliensbachian, 192.9–184.2 Ma) thrusted over the base of the inverted Nindam Fm succession (Yapola gorge; 34.25813°N, 76.83858°E; view to the E). C: Fault-bounded southern contact of the Southern Molasse (LD22-10; n = 24; YSG 82.1 ± 1.9 Ma) overlying the Southern Mélange (Zanskar gorge; 34.044630°N, 77.211740°E; view to the N). D: Successive northward thrusting of the Nindam Fm over the Northern Mélange, which in turn overlies the Dras Volcanics (Takmatchik valley; 34.373180°N, 76.752350°E; view to the SW). E: Serpentinite deposits within the Northern Mélange (Takmatchik valley; 34.372471°N, 76.749214°E). F: Successive northward thrusting of the Nindam Fm over the Northern Mélange, which in turn overlies the Indus Gp (Yapola gorge; 34.323050°N, 76.838360°E; view to the SE). G: Fine-grained turbiditic sequence with interbedded green sandstone and marly shale decametric beds (Chiktan valley; 34.40032°N, 76.52439°E; view to the NE). H: Green sandstone bed base displaying flute cast structures (arrows; Chiktan valley; 34.408020°N, 76.524350°E). I: Representative Chiktan Fm conglomeratic level with boulder-size carbonate clasts reworked from the Lower Cretaceous Khalsi Lst., and rich in Orbitulina sp. (Chiktan valley; 34.457534°N, 76.531908°E, view to the NW). J-K: Middle to Upper Jurassic samples from a lava flow deposit (LD22-75; n = 30; Concordia U-Pb 157.9 ± 0.7 Ma) and a volcaniclastic sandstone (LD22-77; n = 2; YSG 166.2 ± 4.0 Ma) constitutive of the Dras Volcanics (Chiktan valley; 34.44105°N, 76.52659°E, view to the E). L: Fault-bounded northern contact of the Dras Volcanics overlying interbedded sandstone and marly shale levels of the Chiktan Fm (Chiktan valley; 34.447900°N, 76.525460°E; view to the E) M: Contact between the KLB granitoids (*age from Bouilhol et al., 2013) and the onlapping Autochthonous Molasse (Chiktan valley; 34.526595°N, 76.492211°E; view to the NE). N: KLB granitoids (*age from Bouilhol et al., 2013) intruding the older volcanic cover, here represented by the Teah Volcanics (LD19-68; n = 30; Concordia U-Pb 62.9 ± 0.4 Ma; Teah valley; 34.360244°N, 76.970810°E; view to the E). (For interpretation of the references to colour in this figure legend, the reader is referred to the web version of this article.)

setting (i.e., high-energy alluvial and braided fluvial) than the lwr. Indus Gp, on which it unconformably sits. The DZ U-Pb ages retrieved from the Rong Fm (n = 2; 41.3 ± 0.7 Ma; Table 1; Fig. 4) are concordant with the ones reported for the Nimu Fm (41 Ma; Henderson et al., 2010; Wu et al., 2007). However, previously published ^{40}Ar-^{39}Ar geochronology on white micas from the Nimu and Upshi Fms suggest a much younger Oligocene-Miocene age for the upp. Indus Gp (Henderson et al., 2011, 2010), which makes it a lateral equivalent to the Autochthonous Molasse onlapping the KLB (Bhattacharya et al., 2021; Brookfield and Andrews-Speed, 1984; Searle et al., 1990; Zhou et al., 2020).

3.5. Southern units

The Lamayuru Fm was sampled close to the structural contact with the Southern Mélange in the Yapola and Zanskar gorges, where it returned one biostratigraphic (n = 1; 40.6–38 Ma) and one DZ U-Pb age (n = 1; 45.6 ± 1.5 Ma), respectively (Table 1; Fig. 4). These ages complete previously published ones suggesting a continuous deposition of the Lamayuru Fm from the Triassic to Late Eocene. Although more dating is required to confirm this upper limit, our data support previous work stating that the Lamayuru Fm. recorded the pre- and *syn*-collisional deposition onto the Indian margin (Fuchs and Linner, 1995; Robertson and Degnan, 1993; Sinha and Upadhyay, 1993; Upadhyay and Sinha, 1998). They are also consistent with the biostratigraphic (n = 2; 40.1–21 Ma) and DZ U-Pb ages (n = 1; 41.5 ± 1.1 Ma) collected from the overlying Southern Molasse in the Chiktan valley and in Lato (n = 3; 45.2 ± 1.0 Ma; Table 1; Fig. 4).

4. Provenance

4.1. Northern units

Overall, sediments of the Tar Gp, Indus Gp, and Nindam Fm are characterised by εNd values ranging from −6 to 2 (Fig. 5) and a relative enrichment in heavy rare earth elements (HREE; Fig. 6), which links them to a volcanic source rock derived from a depleted upper mantle (e.g., Bayon et al., 2015).

Up-section stratigraphically in the Zanskar gorge, and as already observed by (Clift et al., 2001), the Tar Gp (54–50 Ma) and lwr. Indus Gp (50–21 Ma) show a progressive shift towards more negative εNd values (Fig. 5), light REE (LREE) relative enrichment, and less-pronounced positive Eu anomalies (Supp. Data Fig. S2). The upper levels of the Choksti Fm (45–21 Ma) and overlying Nimu Fm (<21 Ma) are characterised by first occurrence of detrital white micas, becoming more abundant up-section (Henderson et al., 2010). Based on these geochemical characteristics and the increasing number of N-directed paleoflow measured within younger units, some authors have inferred a growing contribution of the Indian plate with time (Clift et al., 2002a, 2001; Henderson et al., 2011, 2010; Sinclair and Jaffey, 2001). However, such interpretation is at odd with the fact that there is a constantly-low amount of Paleozoic DZ in the Choksti and Nimu Fms (Fig. 7), as well as scattered εNd values (Fig. 5). Although a low proportion of Paleozoic DZ could theoretically result from sedimentary recycling or grain-size sorting in distal settings (e.g. Carraro et al., 2025), we consider this unlikely, as both DZ U-Pb spectra and REE patterns from lateral-equivalent formations to the east indicate an Indian input, as discussed below. An alternative explanation for this discrepancy involves discounting the Indian plate as a dominant sediment source and instead attributing the observed isotopic signatures to the temporal evolution of the KLA isotopic compositions. Following Bouilhol et al. (2013), it is proposed that the KLA underwent a shift towards less radiogenic Nd after ca. 50 Ma, potentially driven by changes in subduction-related slab dynamics (Jagoutz et al., 2019). Under this interpretation, the progressive decrease in εNd values recorded in younger sedimentary units would primarily reflect an increasing contribution of post-50 Ma KLA-derived material over time. The observed scatter in εNd values may be attributed to variability in the drainage networks, which alternately eroded and transported detritus from both pre- and post-50 Ma KLA lithologies.

To the east, along the Upshi-Lato section, εNd values are comparable to those of time-equivalent units in the Zanskar gorge (Fig. 5), albeit without a clear stratigraphic trend. A significant Indian plate contribution is attested by the large number of Paleozoic DZ (Fig. 7) incorporated in the Miru Fm (41–32 Ma), Gonmaru La Fm (47–21 Ma), and uppermost Rong Fm (<21 Ma?). We infer that the coeval exhumation (45–30 Ma) of the subducted northern Indian continental margin (Long et al., 2020; St-Onge et al., 2013), now exposed as the Tso Morari dome, has contributed as a source throughout the development of the northwesterly-prograding fluvio-deltaic system of the Indus Gp along this section. Interestingly, the deltaic Miru Fm is less depleted in LREE than the palustrine Gonmaru La Fm (Supp. Data Fig. S2), suggesting a higher contribution from the Indian plate in the more distal units.

The REE patterns of the Nindam Fm closely resemble those measured in the Dras Volcanics (Fig. 6E-F) whilst the dominance of Late Cretaceous DZ U-Pb age populations matches the main magmatic phases of the Dras Volcanics and Kargil Intrusives (Fig. 7). These observations strongly support previously published petrographic, *in-situ* zircon geochemical, and whole-rock geochemical and Nd isotopic data, demonstrating that the Nindam Fm was sourced from the Dras Volcanics (Andjić et al., 2022; Clift et al., 2002b, 2000; Robertson and Degnan, 1994; Walsh et al., 2019). However, contrary to these studies, our new biostratigrahic constraints on the Nindam Fm (41–32 Ma) indicate that the DZ U-Pb ages likely reflect recycled grains from the Dras Volcanics and Kargil Intrusives and therefore do not define a maximum depositional age. Within the Nindam Fm, Indian-derived Paleozoic DZ are only recorded in the Yapola gorge and are less frequent towards the section top (Supp. Data Fig. S4). εNd generally increases both up-section and towards the east (Fig. 5; Supp. Data Fig. S4) whilst HREE are

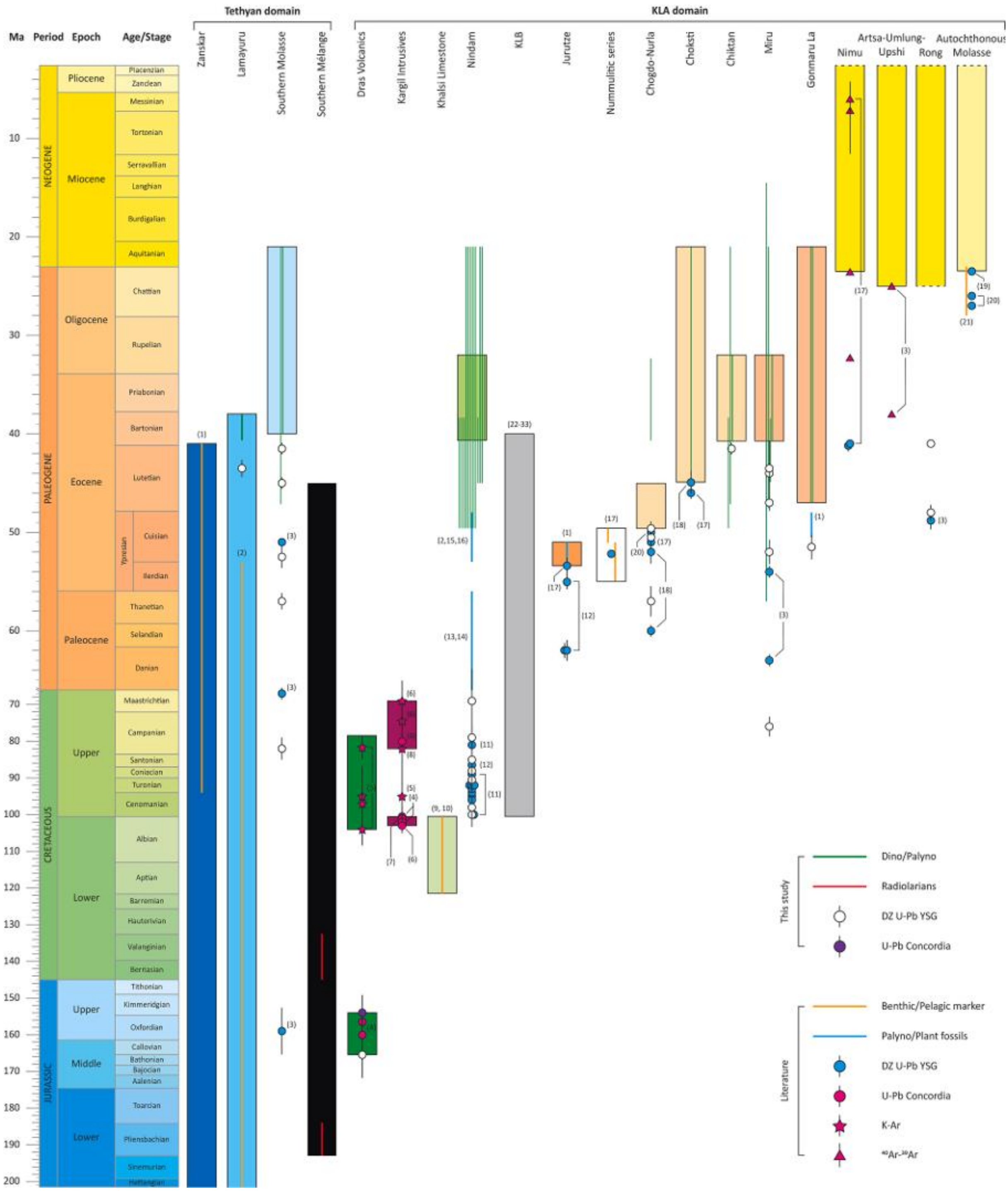

Fig. 4. Chronostratigraphic chart of the ISZ with reported ages from this study and previous work: 1: (Mathur et al., 2009); 2: (Sinha and Upadhyay, 1993); 3: (Henderson et al., 2011); 4: (Walsh et al., 2021); 5: (Reuber, 1989); 6: (Honegger et al., 1982); 7: (Schärer et al., 1984); 8: (Brookfield and Reynolds, 1981); 9: (Mathur and Vogel, 1988); 10: (Tewari et al., 1970); 11: (Walsh et al., 2019); 12: (Andjić et al., 2022); 13: (Upadhyay et al., 2004); 14: (Mathur and Jain, 1980); 15: (Mathur and Juyal, 1996); 16: (Mathur et al., 2008); 17: (Henderson et al., 2010); 18: (Wu et al., 2007); 19: (Zhou et al., 2020); 20: (Bhattacharya et al., 2021); 21: (Bajpai et al., 2004); 22–33: (Borneman et al., 2015; Bosch et al., 2011; Bouilhol et al., 2013, 2011; Clift et al., 2002a; Heuberger et al., 2007; Jagoutz et al., 2019, 2009; Jagoutz and Schmidt, 2012; Lakhan et al., 2020a, 2020b; Ravikant et al., 2009; Saktura et al., 2021; Schaltegger et al., 2002; Shellnutt et al., 2014).

progressively enriched eastward with respect to medium REE (Supp. Data Fig. S4). Together with the consistent absence of post-80 Ma DZ, these observations likely correlate with a decreasing contribution of the Indian plate and a coeval increasing contribution from a more radiogenic pre-50 Ma KLA source (e.g., Dras Volcanics, Kargil Intrusive; Fig. 7). This could be explained by a dilution of Indian-plate sediments as a result of aggradation/progradation of the shallowing-upward Nindam turbiditic system (Clift et al., 2000; Searle et al., 1990).

4.2. Southern units

Contrary to the KLA-derived northern units, the Lamayuru Fm and Southern Molasse show highly negative εNd values comprised between −12 and −8 (Fig. 5), and relatively homogeneous, flat REE patterns

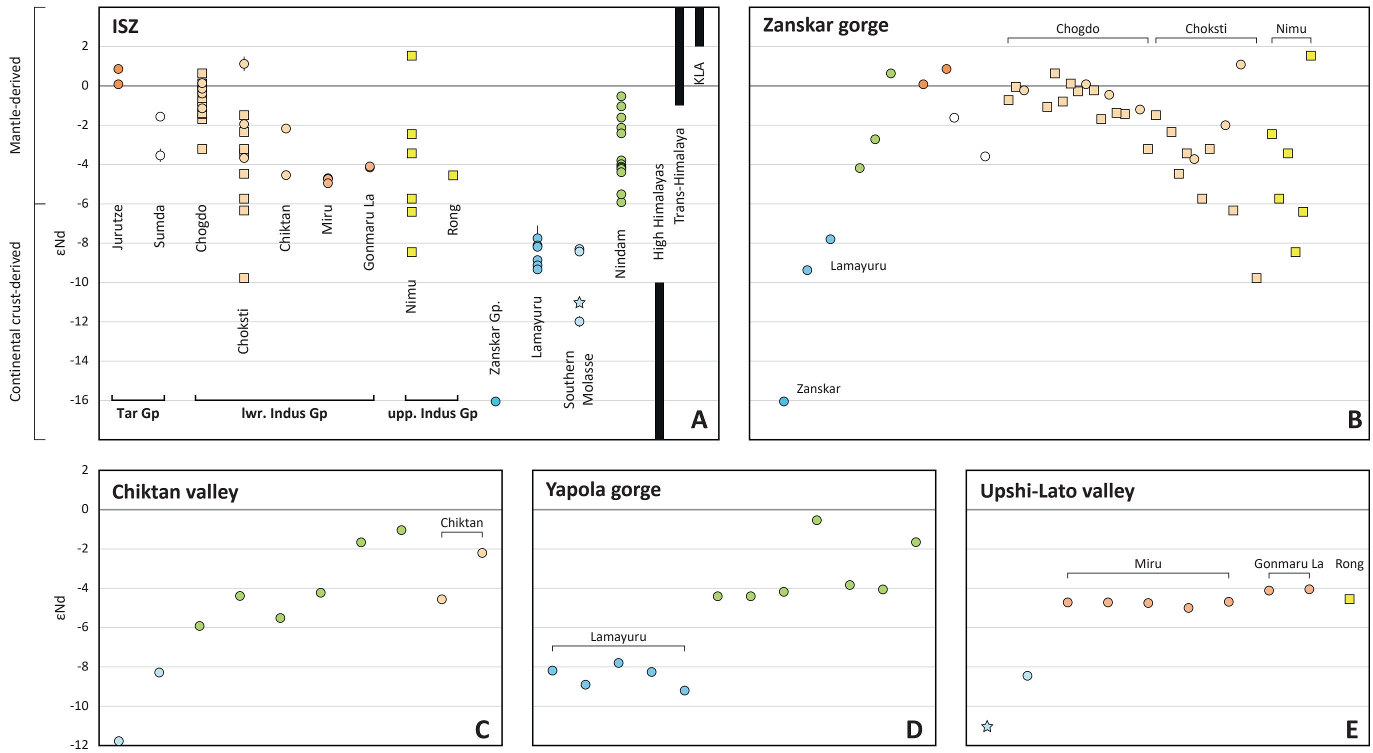

Fig. 5. A: $_{\varepsilon}$Nd values measured within sedimentary formations of the ISZ (circles: this study; squares: Clift et al., 2001; star: Henderson et al., 2011) compared with the measured ranges for the potential sources of the High Himalayas (Allègre and Othman, 1980; Searle et al., 1997), Trans-Himalaya (Allegre and Rousseau, 1988), and the KLA (Bignold et al., 2006; Bouilhol et al., 2011; Dhuime et al., 2009; Heuberger et al., 2007; Jagoutz et al., 2006; Khan et al., 2004; Ravikant et al., 2009; Rolland et al., 2002; Schaltegger et al., 2002). B-E: Stratigraphic evolution of the $_{\varepsilon}$Nd up-section (to the right) along the studied transects.

(Fig. 6). The one sample from the Zanskar Gp, collected in the Zanskar gorge, is characterised by a more negative $_{\varepsilon}$Nd (−16) and a pronounced HREE depletion. The southern units are thus characterised by a significant input from enriched upper continental crust lithologies (Bayon et al., 2015). The high occurrence of Paleozoic DZ points to the Indian plate as the main source of sediments (Fig. 7). Our data support the interpretations of Henderson et al. (2011) who showed that granitic clasts derived from the KLB are rare or absent within the Southern Molasse, ruling out the correlation with the Chogdo Fm made by (Clift et al., 2002a).

A general up-section trend towards higher $_{\varepsilon}$Nd values is observed within the southern units (Fig. 5), implying a growing contribution of the KLA. This observation is supported by SSW-directed paleoflows measured in the uppermost Lamayuru Fm and Southern Molasse, which align with previous results (Clift et al., 2002a; Henderson et al., 2011). The Late Cretaceous and Paleogene main DZ peaks in the Southern Molasse are consistent with a KLA source (Fig. 7). The DZ populations of the sample retrieved from the Lamayuru Fm in the Zanskar gorge indicate provenance from the KLA. However, the lateral correlation, age, and provenance of this formation remain debated, along with the poorly-constrained nature of its contact with underlying Zanskar Gp (Brookfield and Andrews-Speed, 1984; Clift et al., 2002a; Fuchs and Linner, 1995; Henderson et al., 2011; Sterne, 1979). Therefore, we caution against extrapolating these results to the entire Lamayuru Fm, especially as it is interpreted to have been deposited along the North Indian margin and to include units as old as the Triassic.

4.3. Ophiolites contribution

Whole-rock Cr, Ni, and Co concentrations and relative enrichment to Post Archean Australian Shale (Taylor and McLennan, 1985) constitute a robust qualitative proxy of ophiolitic input in the IBSR (Garzanti and Van Haver, 1988; Henderson et al., 2011, 2010). As already observed by these authors, the data show an upward trend in the contribution of ultramafic rocks from ophiolites, from a depleted older Tar Gp to an enriched younger lwr. Indus Gp (Fig. 8; Supp. Data Fig. S5). The southern units display higher concentrations with the highest values being observed in the Southern Mélange. The discrepancy between the uppermost Lamayuru Fm in the Yapola and the Zanskar gorges indicates a localised ophiolite input in the latter, which is further discussed in *section 5.3*. Comparison with the known-compositions of the closest, presentlyexposed ultramafic rocks suggests that either the Southern Mélange, the Spongtang and Nidar Ophiolites, or Thasgam Complex were the most likely sources of Cr, Ni, and Co in the IBSR.

5. Tectono-sedimentary evolution of the ISZ

5.1. Evolution of the foreland basin (ca. < 55 Ma)

The proximal marine Tar Gp (54–50 Ma) deposited on the northern margin of the foreland basin (Fig. 9) where it marks the cessation of plain marine depositional conditions. Accordingly, it mostly contains reworked volcanic lithic fragments from the early basic magmatism of the KLA (80–50 Ma; Garzanti and Van Haver, 1988; Henderson et al., 2010) with no or rare inputs from the Indian plate (Figs. 5 to 7). Thermochronometry data indicate that the collision-induced northward tilting and rapid cooling of the KLA (53–40 Ma) resulted in a rapid exhumation and a high topography along its southern margin (Clift et al., 2002b; Kirstein, 2011; Kumar et al., 2017; Schlup et al., 2003; Tripathy-Lang et al., 2013). The earliest record of this deformation phase is found in the Zanskar gorge where the Chogdo Fm is transgressive over the Sumda Fm (Fig. 2; Clift et al., 2002a; Searle et al., 1990), dating the discordant contact at 51–50 Ma.

The Early-Middle Eocene tectonic uplift of the KLA led to the significant unroofing of its volcanic cover to its deeper granitic roots, mostly occurring between 44 and 25 Ma during a period of exhumation

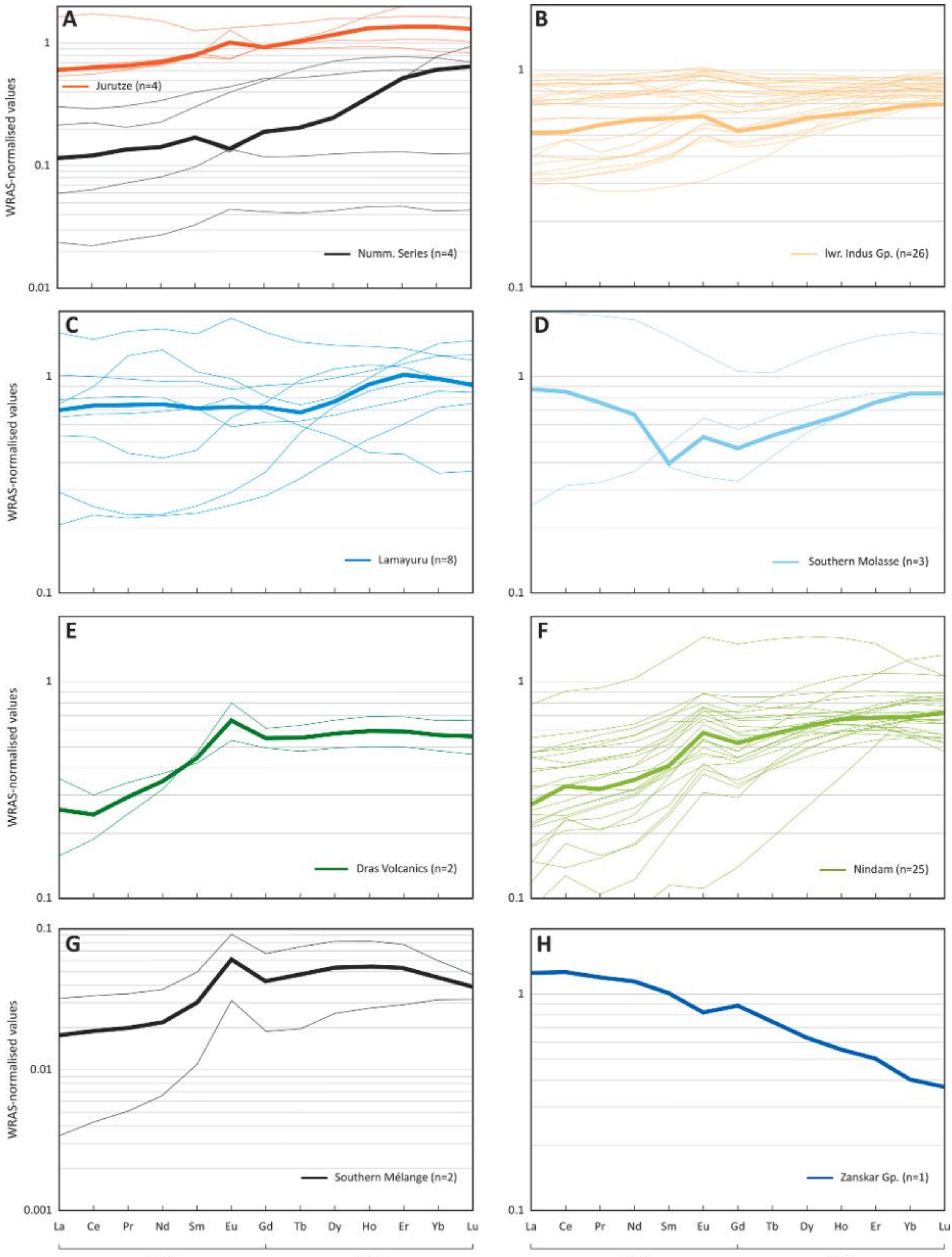

Fig. 6. WRAS-normalised (Bayon et al., 2015) rare earth element diagrams with individual samples (thin lines) and median values (thick lines).

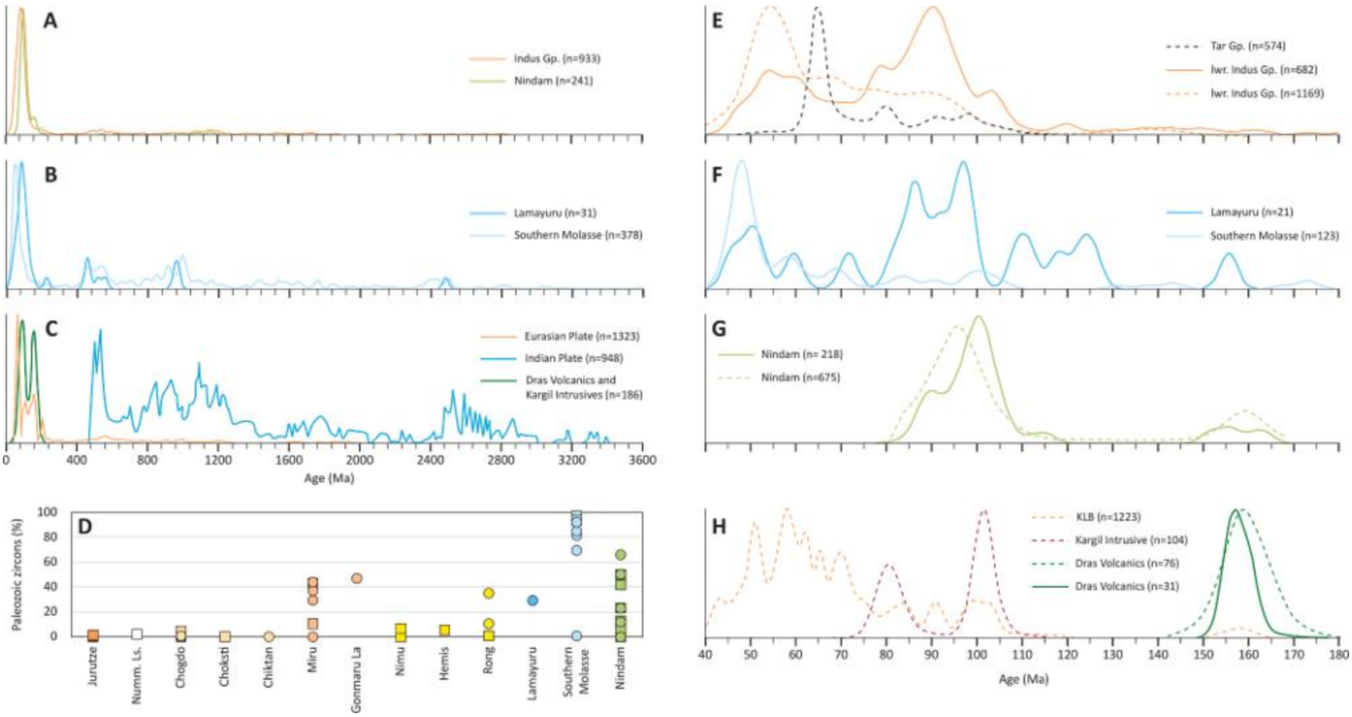

Fig. 7. A-C: Kernel density estimates (i.e., KDEs) of U-Pb DZ ages from the studied formations (A and B) compared with composite samples (C) from previous studies of the Eurasian plate, Indian plate, Dras Volcanics, and Kargil Instrusives. D: Calculated proportions of Indian-derived Paleozoic DZ within formations of the ISZ (circles from this study; squares from the literature). E-G: Same as A to C over the last 180 Ma where U-Pb zircon populations of the studied formations (solid lines) are compared with data from previous work (dotted lines). H: Comparison with the potential sources of the sedimentary formations displayed in E-G. Only grains with $-5 < dc < 10$ were used to generate the KDEs, where dc is the distance to Concordia (Vermeesch, 2021). Published data used to generate the U-Pb age dataset (Supp. Data Table S3) were compiled from: Eurasian plate (Chu et al., 2006; Harrison et al., 2000; Henderson et al., 2011, 2010; Leier et al., 2007; Miller et al., 2000; Murphy et al., 1997; Schärer et al., 1984; Wen et al., 2008; Xu et al., 1985); Indian plate (Gehrels et al., 2003); Dras Volcanics and Kargil Intrusives (Brookfield and Reynolds, 1981; Honegger et al., 1982; Reuber, 1989; Schärer et al., 1984; Sharma et al., 1978; Upadhyay et al., 2004; Walsh et al., 2021, 2019); Tar Gp (Andjić et al., 2022; Henderson et al., 2010); lwr. Indus Gp (Bhattacharya et al., 2021; Henderson et al., 2011, 2010; Wu et al., 2007); Nindam Fm (Andjić et al., 2022; Walsh et al., 2019); and KLB (Borneman et al., 2015; Bosch et al., 2011; Bouilhol et al., 2013, 2011; Clift et al., 2002a; Heuberger et al., 2007; Jagoutz et al., 2019, 2009; Jagoutz and Schmidt, 2012; Lakhan et al., 2020a, 2020b; Ravikant et al., 2009; Saktura et al., 2021; Schaltegger et al., 2002; Shellnutt et al., 2014).

quiescence (Kirstein, 2011; Kumar et al., 2017). During this time, the lwr. Indus Gp (50–21 Ma) deposited in a filling-up foreland basin presenting intermittent shallow marine conditions. In eastern Ladakh, the ongoing exhumation of the Tso Morari Complex (45–30 Ma; St-Onge et al., 2013) partly controlled the sedimentation and drainage patterns as shown by the greater Indian input in sediments along the Upshi-Lato section (Fig. 7, Supp. Data Fig. S2 and S3). In western Ladakh, the KLA was also affected by the Early-Middle Eocene rapid exhumation. Between ca. 40 and 32 Ma, the erosion products of the KLA deposited on its southern edge as the Chiktan Fm, probably within an older intra-arc basin. South of this basin, the coeval dismantlement of the topographic high formed by the uplifted Dras Volcanics and Kargil Intrusives was preserved as the Nindam Fm. This formation only shows a contribution from the Indian plate in the Yapola gorge (Supp. Data Fig. S4; Andjić et al., 2022; Walsh et al., 2019). Overall, these data could suggest that the foreland was not equally wide (Van Haver, 1984) or that distinct sedimentary basins in western and eastern Ladakh were somewhat structurally disconnected at this time (Sutre, 1990; Van Haver, 1984). The latter hypothesis supports a drainage basin feeding the Zanskar valley but not the Yapola gorge with dismantled material from the already-obducted Spongtang Ophiolite (Fig. 8).

Later, the regional kinematic changed when the KLA was tilted southward at 22 Ma, succeeded by the exhumation of its central part (Kirstein, 2011; Kirstein et al., 2006; Kumar et al., 2017; Schlup et al., 2003) and subsequent discordant deposition of the upp. Indus Gp (ca. $<$ 25 Ma) over older units (Fig. 2; Bhattacharya et al., 2020; Clift et al., 2002a; Henderson et al., 2011; Searle et al., 1990; Sinclair and Jaffey, 2001). By this time, the foreland has migrated southward and deposition in the ISZ occurred in a filled-up intermontane setting (Henderson et al., 2010; Searle et al., 1990; Sinclair and Jaffey, 2001).

5.2. Ophiolite emplacement

Three main mafic–ultramafic complexes are present within the ISZ in Ladakh. From east to west: 1) the Nidar Ophiolite (140 ± 32 Ma; Ahmad et al., 2008), which partly preserves the oceanic mantle basement on which arc-derived magmatism developed in the Cretaceous (Buchs, 2019); 2) the Spongtang Ophiolite, which primarily shows the Jurassic (177–160 Ma; Catlos et al., 2019) MOR-type oceanic basement and evidence of intra-oceanic thrusting (Reuber, 1986) with a Cretaceous magmatic overprint (Catlos et al., 2019); 3) and the Thasgam mafic-ultramafics that represent arc-cumulative sequences (Bhat et al., 2025; Reuber et al., 1989) related to the Dras Volcanics (166–148 Ma; this study; Reuber, 1989; Walsh et al., 2021), which witness the earliest volcanic record of the KLA. The observed dismantled blocks of radiolarian cherts (193–133 Ma) preserved within the Southern Mélange, which are coeval with those associated with volcanic products in Nidar (Zyabrev et al., 2008) and Spongtang (Baxter et al., 2010), suggest that they are most likely of similar age to the radiolarian cherts found near Dras, based on their association with volcanics (Bhat et al., 2023). These occurrences, together with the nature and ages of the peroditic complexes, support their lateral equivalence. They further confirm that the ultramafic rocks within the Southern Mélange belong to the arc basement, which was partly incorporated into a subduction-accretion complex (Robertson, 2000; Villalobos-Orchard et al., 2025). Overall, the three peroditic complexes would represent different portion of the arc

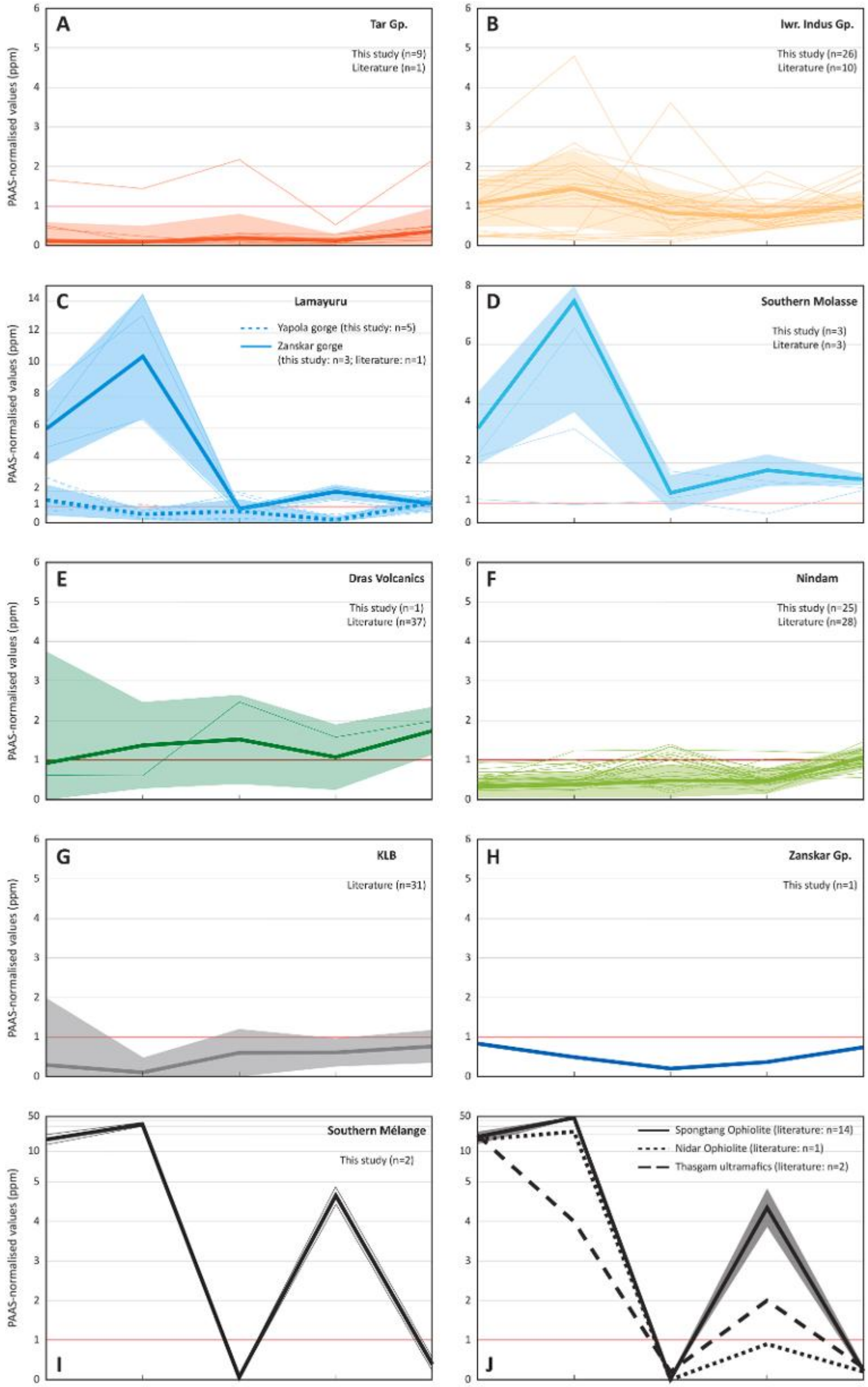

(caption on next page)

Fig. 8. XRF results showing individual samples (thin lines) and median values (thick lines) of trace elements concentrations measured in the IBSR and KLB (A-I) and compared with the closest, presently-exposed ophiolitic ultramafics (J) as potential sources for Cr and Ni enrichment. Because of the limited number of samples analysed in this study, previously published data were also compiled to calculate the more statistically-representative 85th percentile envelopes (shaded areas).All values are normalised to Post Archean Australian Shale (PAAS; (Taylor and McLennan, 1985). Published data used to generate the XRF dataset (Supp. Data Table S4) were compiled from: KLB (Heri et al., 2019; Shellnutt et al., 2014); lwr. Indus Gp (Henderson et al., 2011, 2010; Walsh et al., 2019); Dras Volcanics (Corfield et al., 2001; Walsh et al., 2021, 2019); Southern Molasse (Henderson et al., 2011); Nindam Fm (Clift et al., 2000; Walsh et al., 2019); Southern Mélange (Henderson et al., 2010); Spongtang and Nidar Ophiolites (Mahéo et al., 2004); and Thasgam ultramafics (Bhat et al., 2023).

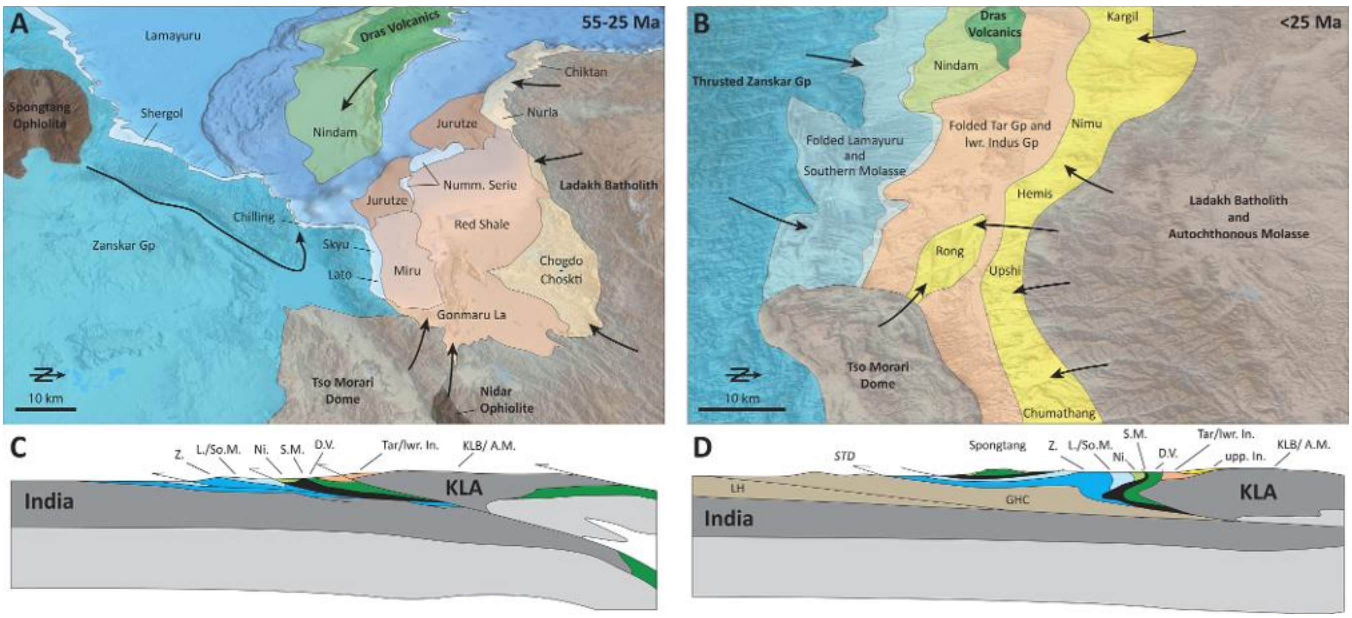

Fig. 9. Schematic reconstruction of the depositional environments for the studied formations of the ISZ in the foreland basin during the Paleogene (A), and in the intermontane basin during the Early Neogene (B). Arrows symbolise major sediment transport pathways from the main respective sources. Time-equivalent cross-section reconstructions (C-D) of the India-KLA collision in Ladakh were modified from (Martin et al., 2025a). Key formations are as follows: Z.– Zanskar Gp; L.– Lamayuru; So.M.– Southern Molasse; Ni.– Nindam; S.M.– Southern Mélange; D.V.– Dras Volcanics; lwr. In.– lwr. Indus Gp; upp. In.– upp. Indus Gp; A.M.– Autochthonous Molasse; GHC– Greater Himalayan Crystalline sequence; LH– Lesser Himalaya; STD– South Tibetan Detachment. Bathymetric maps were made available by EMODnet (https://emodnet.ec.europa.eu/en/), founded by the European Commission Directorate-General for Maritime Affairs and Fisheries (EC DG MARE), and funded by the European Maritime Fisheries and Aquaculture Fund (EMFAF).

system, from the most proximal (Thasgam Complex and Dras Volcanics) to the more distal (Spongtang Ophiolite).

Previous work has used the first occurrence of ultramafic-derived detritus, such as peridotite clasts or high concentration of incompatible elements (e.g. Cr, Ni), to provide a minimum age for the exhumation of the peroditic complexes and possibly ophiolite obduction. In the Indus Basin, the first arrival of ophiolite-derived material is documented in the Zanskar gorge within the Chogdo Fm (49.8 ± 1.2 Ma; Clift et al., 2002a; Garzanti and Van Haver, 1988; Henderson et al., 2011, 2010). The peridotite clasts are relatively unaltered (Clift et al., 2002a; Garzanti and Van Haver, 1988; Henderson et al., 2010), suggesting they were directly derived from ophiolitic sources and not reworked, although the precise source is still to be determined (Henderson et al., 2010). This demonstrates that ophiolitic units were already exhumed and actively eroding during the Early Eocene. Also in the Zanskar gorge, spinel characteristics found within the Southern Mélange (Baxter et al., 2016) more precisely pinpoint to a source dominated by arc-basement rocks (Spongtang or Nidar Ophiolites, showing a wide range of Cr#). However, the timing of emplacement of the Southern Mélange remains uncertain and could not be correlated with the Chogdo Fm, as it may have developed throughout the entire lifespan of the subduction system, from intra-oceanic formation to collision (Robertson, 2000; Villalobos-Orchard et al., 2025). Continued incompatible elemental contribution in the younger Gonmaru La Fm (47–21 Ma), Choksti Fm (45–21 Ma), Chiktan Fm (40–32 Ma), and Southern Molasse (40–21 Ma) indicates a sustained erosion and sediment routing from ophiolitic sources during Late Eocene basin infill (Fig. 8, Supp. Data Fig. S5). In western Ladakh, there is no evidence that the Thasgam Complex and Dras Volcanics sourced any of those ultramafic components, aside from the established contribution to the Nindam Fm. To the east, along the Upshi-Lato section, the Gonmaru La Fm shows a higher proportion of Indian-derived zircons, favouring the Nidar Ophiolite as a principal source.

Overall, despite limited constraints on the precise source, peridotitic components first appear in the sedimentological record at ca. 50 Ma, providing the only robust constraint on the maximum age of ophiolite exhumation. Based on U-Pb dating on zircons, obduction of the Spongtang Ophiolite has been proposed to have occurred between 64.3 ± 0.8 and 42.4 ± 0.5 Ma (Catlos et al., 2019); which is coherent with sedimentological constraints placing it between 56 and 47 Ma (Reuber et al., 1987). Obduction of the Nidar Ophiolite most likely occurred between ca. 49 and 46 Ma (Buchs, 2019). Although timely unresolved, a sequential exhumation is envisioned, whereby the most distal forearc lithosphere (Spongtang Ophiolite) would be obducted first at the onset of continental subduction (55–50 Ma) and feeding the foreland basin. The Nidar Ophiolite exhumation (50–40) followed, before the final uplifting of the arc sequences (Thasgam Complex and Dras Volcanics), which would have eroded and redeposited as the Nindam Fm (<40 Ma). This sequence of ophiolite exhumation would be in line with the general basin evolution.

5.3. Implications for dating the India-KLA collision

The non-consensual geodynamic evolution of the Neo-Tethys, combined with the used of various proxies, led to controversial definitions of collision and its timing (Table 2; Hu et al., 2016), convoluting in a consequent range of possibilities (e.g., Burg and Bouilhol, 2019; Wang et al., 2025). Based on the data collected for this study, we will show hereafter that the stratigraphic record of the ISZ in Ladakh, historically used to benchmark collision, only provides a minimum age for the India-KLA collision.

The IBSR are characterised by an absence of flysch-type, deep marine sediments deposited in a trench setting, potentially suggesting an erosive southern margin of the KLA like the present ones of the western Pacific (Draut and Clift, 2011). A post-80 Ma evolution of the margin toward an erosive one is in line with the geological record. Rare blueschists within the suture are all > 80 Ma (Honegger et al., 1982), and the KLA magmatism show a significant shift in both isotopic composition and latitude after 80 Ma, indicating a greater slab component accompanied by the growth of the arc at the expanse of its back-arc (Burg, 2011; Jagoutz et al., 2019). The preserved molasse correlates with the formation of the foreland basin and tectonic uplift caused by compressional processes during the India-KLA collision (Le Fort, 1989). Accordingly, the minimum age for collision in the ISZ is constrained by the oldest Jurutze Fm (53.4 ± 1.4 Ma; Henderson et al., 2010), whilst subsequent uplift of the KLA is constrained at 53 Ma by thermochronometry and at 51–50 Ma by structural data. Although more speculative, the minimum age for the collision is broadly consistent with the timing of obduction of the Spongtang Ophiolite onto the Indian continental passive margin (64–42 Ma; Catlos et al., 2019), and subsequent arrival of ophiolite-derived sediments in the ITZ (49.8 ± 1.2 Ma, Chogdo Fm).

Table 2
Summary of methods used and published ages for the India-Asia collision (based on the review of Hu et al., 2016).

Methods	Rationale	Limitations	Age (Ma)
Regional unconformities	Abrupt sedimentary changes marks the onset of post-collision sedimentation	Can be influenced by other factors (e.g., tectonics, magmatism, sea-level changes) as observed in passive margins	70–50
Stratigraphy and sedimentology	Asian detritus on the Indian plate marks the onset of post-collision sedimentation	Depends on provenance, location, and preservation of sediments but constitute a reliable tool to date the onset of collision	59 ± 1
Tectonics of sedimentary basins	Transition from passive-margin to *syn*-collisional sedimentation marks the onset of collision	Can occur later but, coupled with robust stratigraphic and provenance data, is a reliable tool to date the onset of collision	56–49
Cessation of marine sedimentation	The closing of the Neo Tethys marks the onset of the collision	Only gives a minimum age for collision as marine conditions can persist long after collision	52.8–34
Intermontane sedimentation	Terrestrial deposits in the suture zone marks the onset of post-collision sedimentation	Provides insights into the syn- and post-collisional evolution of the orogenic belt rather than the initial collision timing.	45–18
Convergence rate	Deceleration in India-Asia convergence marks the onset of collision	Can be influenced by other factors (e.g., slab break-off, Deccan's plume weaking…)	60–47
Magmatism	Changes in magmatic signatures marks the onsent of continental subduction	Can be influenced by other factors (e.g., delayed change of magmatic composition, slab break-off)	55–50
Continental deformation	Early fold-thrust deformation and metamorphism indicate collision-related deformation	Only gives a minimum age for collision and can be influenced by other factors (e.g., ophiolite subduction, arc-continent collision)	54–44
HP and UHP metamorphism	HP and UHP rocks marks the onsent of continental subduction	Assumes that India subducted under Asia and not under an intervening oceanic arc but constitute a a reliable tool to date the onset of collision	53–46
Paleomagnetism	Overlap of paleolatitude data from both plates marks the onset of collision	Provides a minimum age but constitute a reliable tool to date the onset of collision	52 ± 4

The dating of oldest sediments showing a mixed provenance, marking the first arrival of Asian-derived sediments onto the Indian plate, has also been used to constrain the timing of the collision. However, previous work in the Himalayas has revealed that such change occurs earlier within a deep trench setting (59 ± 1 Ma; Hu et al., 2015) than shallower ones (54 Ma; Najman et al., 2017). The relevance of such proxy in deep depositional environments relies on the assumption that the investigated turbidites were not deposited over great distances onto to the ocean floor. However, some are known to travel further than 750 km from their source (Heezen et al., 1954), and can thus record provenance changes before continent–continent collision. In contrast, shallower sediments are subject to incomplete record (e.g., IBSR) and are distant from the trench, which can delay the archiving of collisional suturing. Furthermore, mixed provenance data in shallow formations might be overprinted by a dominant signal from their close source through allochthonous sediments dilution. These observations are supported by the discrepant provenance data in Ladakh, in particular for the Tar Gp and Nindam Fm (Figs. 5 to 8). The use of DZ U-Pb data for dating sediments is hampered by numerous pre-requisites, including the rarity of young grains and their potential dilution in large sediment-routing systems (e.g., Sharman and Malkowski, 2020). Our data shows that main difficulties in the ISZ are linked to the Late Eocene dismantlement (Nindam Fm, 41–32 Ma) of an older Cretaceous source (Dras Volcanics and Kargil Instrusives, 165–70 Ma; Fig. 4), and coeval cessation of an active volcanism (ca. 40 Ma; Bouilhol et al., 2013) to provide contemporaneous zircon grains (e.g., upp. Indus Gp; Fig. 4).

Finally, the timing of the cessation of plain marine conditions differs within the foreland basin. The upper limit of the Tar Gp (50 Ma, Numm. Ls; Henderson et al., 2010) indicates that continental sedimentation on the foreland northern margin started ca. 10 Ma earlier than on the southern margin, where it is constrained at the contact between the uppermost Lamayuru Fm and the overlying Southern Molasse (ca. 40 Ma). The diachronic infill of the foreland basin is consistent with the development of an Early Eocene foredeep (Ali et al., 2025; Robertson and Degnan, 1994). Palynological data support previous sedimentological work on the lwr. Indus Gp depositional environments, showing that coastal and shallow marine conditions were periodically maintained throughout the Paleogene. Such persisting seaways rule out last marine deposits as reliable markers for continent–continent collision (Hu et al., 2016).

6. Conclusions

This study provides a revised tectonostratigraphic framework for the Indus Suture Zone in Ladakh, NW India, based on a multi-proxy approach. The main conclusions are:

1. **Jurassic arc development**. New U-Pb ages for the Dras Volcanics (Concordia age = 157.94 ± 0.7 Ma; YSG age = 166.2 ± 4 Ma)

confirm the early development of the intra-oceanic KLA during the Middle to Upper Jurassic onto an oceanic basement, partly preserved in the Southern Mélange.
2. **Revised age of the Nindam Fm**. New biostratigaphic data place deposition of the Nindam Fm in the Late Eocene (40.6–32.3 Ma) rather than the previously assumed Cretaceous. The observed DZ U-Pb ages reflect recycled grains from its primary Dras Volcanics and Kargil Intrusives sources. The IBSR thus exclusively record the Paleogene-Neogene foreland sedimentation (< 53.4 ± 1.4 Ma), providing a minimum age for the India-KLA collision.
3. **Diachronous marine retreat**. Plain marine conditions ceased earlier along the northern margin of the foredeep (50 Ma) than along its southern margin (40 Ma). The last occurrence of marine deposits therefore does not constitute a reliable marker for collision onset.
4. **Multi-stage tectonic control on sedimentation**. Provenance evolution records successive tectonic processes, which collectively governed sediment routing in the foreland, including collision-induced uplift and unroofing of the KLA (53–40 Ma and < 25 Ma), Spongtang Ophiolite obduction onto the Indian margin (64–42 Ma), southward thrusting of the Nidar Ophiolite (49–46 Ma), exhumation of the Tso Morari Complex (45–30 Ma), and final backthrusting (< 23 Ma).

Despite unpromising previous attempts, this study is the first to demonstrate that extensive palynological analyses are both feasible effective to robustly refine the tectonostratigraphic history of the region. Renewed investigations, especially in eastern Ladakh and within the Indian-margin flysch deposits of the Lamayuru Fm, have strong potential to provide further insight into the geodynamic evolution of the India-Asia collision. More generally, this study highlights the potential of Himalayan sedimentary basins as archives of orogenic processes, recording the temporal and spatial evolution of multi-stage tectonic events during continental collision.

Data availability statement

All data supporting the findings of this study are available within the paper and its Supplementary Information files.

CRediT authorship contribution statement

Lucas Vimpere: Writing – review & editing, Writing – original draft, Visualization, Supervision, Resources, Project administration, Methodology, Investigation, Funding acquisition, Formal analysis, Conceptualization. **Pierre Bouilhol:** Writing – review & editing, Resources, Project administration, Methodology, Investigation, Funding acquisition, Formal analysis, Conceptualization. **Pietro Sternai:** Writing – review & editing, Resources, Methodology, Investigation, Conceptualization. **Speranta-Maria Popescu:** Writing – review & editing, Resources, Methodology, Investigation, Formal analysis. **Jean-Pierre Suc:** Writing – review & editing, Resources, Methodology, Investigation, Formal analysis. **Spela Gorican:** Writing – review & editing, Resources, Methodology, Investigation, Formal analysis. **Marc Poujol:** Writing – review & editing, Resources, Methodology, Investigation, Formal analysis. **Nathan Cogné:** Writing – review & editing, Resources, Methodology, Investigation, Formal analysis. **Germain Bayon:** Resources, Methodology, Investigation, Formal analysis. **Anne Trinquier:** Resources, Methodology, Investigation, Formal analysis. **Thierry Adatte:** Writing – review & editing, Resources, Methodology, Investigation, Formal analysis. **Jorge E. Spangenberg:** Writing – review & editing, Resources, Methodology, Investigation, Formal analysis. **Marcel Regelous:** Writing – review & editing, Resources, Methodology, Investigation, Formal analysis. **Christian Vérard:** Writing – review & editing, Visualization, Software, Resources. **Rajeev Upadhyay:** Supervision. **Sébastien Castelltort:** Writing – review & editing, Resources, Project administration, Methodology, Investigation, Funding acquisition, Conceptualization.

Declaration of Competing Interest

The authors declare that they have no known competing financial interests or personal relationships that could have appeared to influence the work reported in this paper.

Acknowledgments

We convey our gratitude to C.P. Dorjay, Karma Topgyal, Norbu, Sia-La Guest House staff, Denis Vimpere, and Didier Vimpere for their invaluable logistical help during fieldwork. We thank François Gischig and Malik Meghazi (University of Geneva) for thin-section manufacturing. We would like to acknowledge Peter D. Clift for sharing Nd-isotopic results and the location of samples from a previous expedition. We are grateful to the editor and three anonymous reviewers for their constructive comments on earlier versions of the manuscript. This research was funded by the Department of Earth Sciences of the University of Geneva, Foundation Ernest Boninchi, and Foundation Ernst and Lucie Schmidheiny.

Appendix A. Supplementary data

Supplementary data to this article can be found online at https://doi.org/10.1016/j.gr.2026.03.014.

References

Ahmad, T., Tanaka, T., Sachan, H.K., Asahara, Y., Islam, R., Khanna, P.P., 2008. Geochemical and isotopic constraints on the age and origin of the Nidar Ophiolitic complex, Ladakh, India: Implications for the Neo-Tethyan subduction along the Indus suture zone. Tectonophysics 451, 206–224. https://doi.org/10.1016/j.tecto.2007.11.049.

Aitchison, J.C., Badengzhu, Davis, A.M., Liu, J., Luo, H., Malpas, J.G., McDermid, I.R.C., Wu, H., Ziabrev, S.V., Zhou, M., 2000. Remnants of a Cretaceous intra-oceanic subduction system within the Yarlung–Zangbo suture (southern Tibet). Earth Planet. Sci. Lett. 183, 231–244. 10.1016/S0012-821X(00)00287-9.

Ali, N., Hanif, M., Mohibullah, M., Khan, A., Orakzai, A., Hashmi, S.I., 2025. On the transition from Remnant Tethys Sea to Foreland Basin during the late Paleogene in the Western Himalayas. Pakistan. Geol. J. 60, 2351–2379. https://doi.org/10.1002/gj.5176.

Allègre, C.J., Othman, D.B., 1980. Nd–Sr isotopic relationship in granitoid rocks and continental crust development: a chemical approach to orogenesis. Nature 286, 335–342. https://doi.org/10.1038/286335a0.

Allegre, C.J., Rousseau, D., 1988. Nd-Sr isotopic study of Himalaya tibet gneiss and granitoids. Development of the asian continental crust since the jurassic time. Int. Congr. Geochem. Cosmochem. 70, 66. https://doi.org/10.1016/0009-2541(88)90375-0.

Andjić, G., Zhou, R., Jonell, T.N., Aitchison, J.C., 2022. A Single Dras-Kohistan-Ladakh Arc Revealed by Volcaniclastic Records. Geochem. Geophys. Geosystems 23. https://doi.org/10.1029/2021GC010042.

Bajpai, S., Whatley, R.C., Prasad, G.V.R., Whittaker, J.E., 2004. An Oligocene non-marine ostracod fauna from the Basgo Formation (Ladakh Molasse), NW Himalaya. India. J. Micropalaeontology 23, 3–9. https://doi.org/10.1144/jm.23.1.3.

Baxter, A.T., Aitchison, J.C., Ali, J.R., Chan, J.-S.-L., Chan, G.H.N., 2016. Detrital chrome spinel evidence for a Neotethyan intra-oceanic island arc collision with India in the Paleocene. J. Asian Earth Sci. 128, 90–104. https://doi.org/10.1016/j.jseaes.2016.06.023.

Baxter, A.T., Aitchison, J.C., Ali, J.R., Zyabrev, S.V., 2010. Early cretaceous radiolarians from the Spongtang massif, Ladakh, NW India: implications for Neo-Tethyan evolution. J. Geol. Soc. 167, 511–517. https://doi.org/10.1144/0016-76492009-099.

Bayon, G., Toucanne, S., Skonieczny, C., André, L., Bermell, S., Cheron, S., Dennielou, B., Etoubleau, J., Freslon, N., Gauchery, T., Germain, Y., Jorry, S.J., Ménot, G., Monin, L., Ponzevera, E., Rouget, M.-L., Tachikawa, K., Barrat, J.A., 2015. Rare earth elements and neodymium isotopes in world river sediments revisited. Geochim. Cosmochim. Acta 170, 17–38. https://doi.org/10.1016/j.gca.2015.08.001.

Beck, R.A., Burbank, D.W., Sercombe, W.J., Riley, G.W., Barndt, J.K., Berry, J.R., Afzal, J., Khan, A.M., Jurgen, H., Metje, J., Cheema, A., Shafique, N.A., Lawrence, R. D., Khan, M.A., 1995. Stratigraphic evidence for an early collision between northwest India and Asia. Nature 373, 55–58. https://doi.org/10.1038/373055a0.

Bhat, I., Chauhan, H., Ahmad, T., 2025. Supra-subduction Zone Arc Magmatism along the Indus Suture Zone (ISZ), Western Ladakh: Implications from Clinopyroxene Chemistry of the Thasgam Ophiolitic Slice. J. Geol. Soc. India 101, 827–831. 10.17491/jgsi/2025/174168.

Bhat, I.M., Chauhan, H., Ahmad, T., Dar, R.A., 2023. Geochemistry and petrogenesis of ophiolitic rocks from the Indus Suture Zone (ISZ), Ladakh Himalaya: insights for depleted mantle beneath an intra-oceanic island arc complex. Int. Geol. Rev. 65, 3329–3347. https://doi.org/10.1080/00206814.2023.2185824.

Bhattacharya, G., Robinson, D.M., Orme, D.A., Najman, Y., Carter, A., 2020. Low-Temperature Thermochronology of the Indus Basin in Central Ladakh, Northwest India: Implications of Miocene-Pliocene Cooling in the India-Asia Collision Zone. Tectonics 39, e2020TC006333. https://doi.org/10.1029/2020TC006333.

Bhattacharya, G., Robinson, D.M., Wielicki, M.M., 2021. Detrital zircon provenance of the Indus Group, Ladakh, NW India: Implications for the timing of the India-Asia collision and other syn-orogenic processes. GSA Bull. 133, 1007–1020. https://doi.org/10.1130/B35624.1.

Bhutani, R., Pande, K., Venkatesan, T.R., 2009. 40Ar–39Ar dating of volcanic rocks of the Shyok suture zone in north–west trans-Himalaya: Implications for the post-collision evolution of the Shyok suture zone. J. Asian Earth Sci. 34, 168–177. https://doi.org/10.1016/j.jseaes.2008.03.013.

Bignold, S.M., Treloar, P.J., Petford, N., 2006. Changing sources of magma generation beneath intra-oceanic island arcs: an insight from the juvenile Kohistan island arc, Pakistan Himalaya. Chem. Geol. 233, 46–74. https://doi.org/10.1016/j.chemgeo.2006.02.008.

Borneman, N.L., Hodges, K.V., Van Soest, M.C., Bohon, W., Wartho, J.-A., Cronk, S.S., Ahmad, T., 2015. Age and structure of the Shyok suture in the Ladakh region of northwestern India: Implications for slip on the Karakoram fault system: AGE OF SHYOK SUTURE. Tectonics 34, 2011–2033. https://doi.org/10.1002/2015TC003933.

Bosch, D., Garrido, C.J., Bruguier, O., Dhuime, B., Bodinier, J.-L., Padròn-Navarta, J.A., Galland, B., 2011. Building an island-arc crustal section: Time constraints from a LA-ICP-MS zircon study. Earth Planet. Sci. Lett. 309, 268–279. https://doi.org/10.1016/j.epsl.2011.07.016.

Bouilhol, P., Jagoutz, O., Hanchar, J.M., Dudas, F.O., 2013. Dating the India–Eurasia collision through arc magmatic records. Earth Planet. Sci. Lett. 366, 163–175. https://doi.org/10.1016/j.epsl.2013.01.023.

Bouilhol, P., Schaltegger, U., Chiaradia, M., Ovtcharova, M., Stracke, A., Burg, J.-P., Dawood, H., 2011. Timing of juvenile arc crust formation and evolution in the Sapat complex (Kohistan–Pakistan). Chem. Geol. 280, 243–256. https://doi.org/10.1016/j.chemgeo.2010.11.013.

Brookfield, M.E., Andrews-Speed, C.P., 1984. Sedimentology, petrography and tectonic significance of the shelf, flysch and molasse clastic deposits across the Indus Suture Zone, Ladakh, NW India. Sediment. Geol. 40, 249–286. https://doi.org/10.1016/0037-0738(84)90011-3.

Brookfield, M.E., Reynolds, P.H., 1981. Late cretaceous emplacement of the Indus suture zone ophiolitic mélanges and an Eocene-Oligocene magmatic arc on the northern edge of the Indian plate. Earth Planet. Sci. Lett. 55, 157–162. https://doi.org/10.1016/0012-821X(81)90094-7.

Buchs, N., 2019. Geology of the Nidar-Tso Morari area (Indian Himalayas, Ladakh): from intra-oceanic subduction to nappe exhumation (Doctoral dissertation). Université de Lausanne, Lausanne.

Burg, J.-P., 2011. The Asia–Kohistan–India Collision: Review and Discussion, in: Arc-Continent Collision, Frontiers in Earth Sciences. Springer Berlin Heidelberg, Berlin, Heidelberg, pp. 279–309. 10.1007/978-3-540-88558-0_10.

Burg, J.-P., Bouilhol, P., 2019. Timeline of the South Tibet – Himalayan belt: the geochronological record of subduction, collision, and underthrusting from zircon and monazite U–Pb ages. Can. J. Earth Sci. 56, 1318–1332. https://doi.org/10.1139/cjes-2018-0174.

Carraro, D., Gaynor, S.P., Ventra, D., Ulyanov, A., Moscariello, A., 2025. Testing the fidelity of zircon as a provenance indicator in fluvial-fan successions: an example from the Palaeogene Colton Formation, Central Utah, USA. Depositional Rec. 11, 511–536. https://doi.org/10.1002/dep2.316.

Catlos, E.J., Pease, E.C., Dygert, N., Brookfield, M., Schwarz, W.H., Bhutani, R., Pande, K., Schmitt, A.K., 2019. Nature, age and emplacement of the Spongtang ophiolite, Ladakh, NW India. J. Geol. Soc. 176, 284–305. https://doi.org/10.1144/jgs2018-085.

Chu, M.-F., Chung, S.-L., Song, B., Liu, D., O'Reilly, S.Y., Pearson, N.J., Ji, J., Wen, D.-J., 2006. Zircon U-Pb and Hf isotope constraints on the Mesozoic tectonics and crustal evolution of southern Tibet. Geology 34, 745. https://doi.org/10.1130/G22725.1.

Clift, P.D., Carter, A., Krol, M., Kirby, E., 2002a. Constraints on India-Eurasia collision in the Arabian Sea region taken from the Indus Group, Ladakh Himalaya. India. Geol. Soc. Lond. Spec. Publ. 195, 97–116. https://doi.org/10.1144/GSL.SP.2002.195.01.07.

Clift, P.D., Degnan, P.J., Hannigan, R., Blusztajn, J., 2000. Sedimentary and geochemical evolution of the Dras forearc basin, Indus suture, Ladakh Himalaya. India. Geol. Soc. Am. Bull. 112, 450–466.

Clift, P.D., Hannigan, R., Blusztajn, J., Draut, A.E., 2002b. Geochemical evolution of the Dras-Kohistan Arc during collision with Eurasia: evidence from the Ladakh Himalaya. India. Isl. Arc 11, 255–273. https://doi.org/10.1046/j.1440-1738.2002.00371.x.

Clift, P.D., Shimizu, N., Layne, G.D., Blusztajn, J., 2001. Tracing patterns of erosion and drainage in the Paleogene Himalaya through ion probe Pb isotope analysis of detrital K-feldspars in the Indus Molasse. India. Earth Planet. Sci. Lett. 188, 475–491. https://doi.org/10.1016/S0012-821X(01)00346-6.

Corfield, R.I., Searle, M.P., 2000. Crustal shortening estimates across the north Indian continental margin, Ladakh, NW India. Geol. Soc. Lond. Spec. Publ. 170, 395–410. https://doi.org/10.1144/GSL.SP.2000.170.01.21.

Corfield, R.I., Searle, M.P., Pedersen, R.B., 2001. Tectonic setting, Origin, and Obduction history of the Spontang Ophiolite, Ladakh Himalaya, NW India. J. Geol. 109, 715–736. https://doi.org/10.1086/323191.

Dhuime, B., Bosch, D., Garrido, C.J., Bodinier, J.-L., Bruguier, O., Hussain, S.S., Dawood, H., 2009. Geochemical Architecture of the Lower- to Middle-crustal section of a Paleo-island Arc (Kohistan complex, Jijal–Kamila Area, Northern Pakistan): Implications for the Evolution of an Oceanic Subduction Zone. J. Petrol. 50, 531–569. https://doi.org/10.1093/petrology/egp010.

Draut, A.E., Clift, P.D., 2011. Basins in arc-continent collisions, in: Busby, C., Azor, A. (Eds.), Tectonics of Sedimentary Basins: Recent Advances. Wiley, pp. 347–368. 10.1002/9781444347166.ch17.

Frank, W., Gansser, A., Trommsdorff, V., 1977. Geological observations in the Ladakh area (Himalayas) : a preliminary repor. Schweiz Miner. Petrogr Mitt 57, 89–113. https://doi.org/10.5169/SEALS-44424.

Fuchs, G., 1986. The geology of the Markha-Khurnak region in Ladakh (India). Jahrb. Geol. Bundesanst. 128, 4.

Fuchs, G., 1984. Note on the Geology of the Markha-Nimaling Area in Ladakh (India). Jahrb. Geol. Bundesanst. 127, 5–12.

Fuchs, G., 1979. On the Geology of Western Ladakh. Jahrb. Geol. Bundesanst. 122, 513–540.

Fuchs, G., 1977. Traverse of Zanskar from the Indus to the Valley of Kashmir — a preliminary note. Jahrb. Geol. Bundesanst. 120, 219–229.

Fuchs, G., Linner, M., 1995. Geological Traverse across the Western Himalaya – a Contribution to the Geology of Eastern Ladakh, Lahul, and Chamba. Jahrb. Geol. Bundesanst. 138, 655–685.

Garzanti, E., Baud, A., Mascle, G., 1987. Sedimentary record of the northward flight of India and its collision with Eurasia (Ladakh Himalaya, India). Geodin. Acta 1, 297–312. https://doi.org/10.1080/09853111.1987.11105147.

Garzanti, E., Van Haver, T., 1988. The indus clastics: forearc basin sedimentation in the Ladakh Himalaya (India). Sediment. Geol. 59, 237–249. https://doi.org/10.1016/0037-0738(88)90078-4.

Gehrels, G.E., DeCelles, P.G., Martin, A., Ojha, T.P., Pinhassi, G., Upreti, B.N., 2003. Initiation of the Himalayan orogen as an early Paleozoic thin-skinned thrust belt. GSA Today 13, 4–9.

Green, O.R., Searle, M.P., Corfield, R.I., Corfield, R.M., 2008. Cretaceous-Tertiary Carbonate Platform Evolution and the Age of the India-Asia Collision along the Ladakh Himalaya (Northwest India). J. Geol. 116, 331–353. https://doi.org/10.1086/588831.

Gupta, V.J., Kumar, S., 1975. Geology of Ladakh, Lahaul and spiti regions of Himalaya with special reference to the stratigraphic position of flysch deposits. Geol. Rundsch. 64, 540–563. https://doi.org/10.1007/BF01820682.

Harrison, T.M., Yin, A., Grove, M., Lovera, O.M., Ryerson, F.J., Zhou, X., 2000. The Zedong Window: a record of superposed Tertiary convergence in southeastern Tibet. J. Geophys. Res. Solid Earth 105, 19211–19230. https://doi.org/10.1029/2000JB900078.

Heezen, B.C., Ericson, D.B., Ewing, M., 1954. Further evidence for a turbidity current following the 1929 Grand banks earthquake. Deep Sea Res. 1953 (1), 193–202. https://doi.org/10.1016/0146-6313(54)90001-5.

Henderson, A.L., Najman, Y., Parrish, R., BouDagher-Fadel, M., Barford, D., Garzanti, E., Andò, S., 2010. Geology of the Cenozoic Indus Basin sedimentary rocks: Paleoenvironmental interpretation of sedimentation from the western Himalaya during the early phases of India-Eurasia collision. Tectonics 29, n/a-n/a. https://doi.org/10.1029/2009TC002651.

Henderson, A.L., Najman, Y., Parrish, R., Mark, D.F., Foster, G.L., 2011. Constraints to the timing of India–Eurasia collision; a re-evaluation of evidence from the Indus Basin sedimentary rocks of the Indus–Tsangpo Suture Zone, Ladakh. India. Earth-Sci. Rev. 106, 265–292. https://doi.org/10.1016/j.earscirev.2011.02.006.

Heri, A.R., Bahl, J., Villa, I.M., 2019. Geochemical discrimination and petrogenetic affinities of dykes intruding the Ladakh batholith, NW India. Geol. Soc. Lond. Spec. Publ. 481, 231–250. https://doi.org/10.1144/SP481-2017-150.

Heuberger, S., Schaltegger, U., Burg, J.-P., Villa, I.M., Frank, M., Dawood, H., Hussain, S., Zanchi, A., 2007. Age and isotopic constraints on magmatism along the Karakoram-Kohistan Suture Zone, NW Pakistan: evidence for subduction and continued convergence after India-Asia collision. Swiss J. Geosci. 100, 85–107. https://doi.org/10.1007/s00015-007-1203-7.

Honegger, K., Dietrich, V., Frank, W., Gansser, A., Thöni, M., Trommsdorff, V., 1982. Magmatism and metamorphism in the Ladakh Himalayas (the Indus-Tsangpo suture zone). Earth Planet. Sci. Lett. 60, 253–292. https://doi.org/10.1016/0012-821X(82)90007-3.

Hu, X., Garzanti, E., Moore, T., Raffi, I., 2015. Direct stratigraphic dating of India-Asia collision onset at the Selandian (middle Paleocene, 59 ± 1 Ma). Geology 43, 859–862. https://doi.org/10.1130/G36872.1.

Hu, X., Garzanti, E., Wang, J., Huang, W., An, W., Webb, A., 2016. The timing of India-Asia collision onset – Facts, theories, controversies. Earth-Sci. Rev. 160, 264–299. https://doi.org/10.1016/j.earscirev.2016.07.014.

Jadoon, U.K., Ding, L., Baral, U., Qasim, M., 2020. Early cretaceous to Eocene magmatic records in Ladakh arc: Constraints from U–Pb ages of Deosai volcanics, northern Pakistan. Geol. J. 55, 5384–5397. https://doi.org/10.1002/gj.3730.

Jagoutz, O., Bouilhol, P., Schaltegger, U., Müntener, O., 2019. The isotopic evolution of the Kohistan Ladakh arc from subduction initiation to continent arc collision. Geol. Soc. Lond. Spec. Publ. 483, 165–182. https://doi.org/10.1144/SP483.7.

Jagoutz, O., Muntener, O., Burg, J., Ulmer, P., Jagoutz, E., 2006. Lower continental crust formation through focused flow in km-scale melt conduits: the zoned ultramafic bodies of the Chilas complex in the Kohistan island arc (NW Pakistan). Earth Planet. Sci. Lett. 242, 320–342. https://doi.org/10.1016/j.epsl.2005.12.005.

Jagoutz, O., Schmidt, M.W., 2012. The formation and bulk composition of modern juvenile continental crust: the Kohistan arc. Chem. Geol. 298–299, 79–96. https://doi.org/10.1016/j.chemgeo.2011.10.022.

Jagoutz, O.E., Burg, J.-P., Hussain, S., Dawood, H., Pettke, T., Iizuka, T., Maruyama, S., 2009. Construction of the granitoid crust of an island arc part I: geochronological and geochemical constraints from the plutonic Kohistan (NW Pakistan). Contrib. Mineral. Petrol. 158, 739–755. https://doi.org/10.1007/s00410-009-0408-3.
Khan, S.D., Stern, R.J., Manton, M.I., Copeland, P., Kimura, J.I., Khan, M.A., 2004. Age, geochemical and Sr–Nd–Pb isotopic constraints for mantle source characteristics and petrogenesis of Teru Volcanics, Northern Kohistan Terrane, Pakistan. Tectonophysics 393, 263–280. https://doi.org/10.1016/j.tecto.2004.07.038.
Kirstein, L.A., 2011. Thermal evolution and exhumation of the Ladakh Batholith, northwest Himalaya, India. Tectonophysics 503, 222–233. https://doi.org/10.1016/j.tecto.2011.03.005.
Kirstein, L.A., Sinclair, H., Stuart, F.M., Dobson, K., 2006. Rapid early Miocene exhumation of the Ladakh batholith, western Himalaya. Geology 34, 1049. https://doi.org/10.1130/G22857A.1.
Kumar, R., Jain, A.K., Lal, N., Singh, S., 2017. Early–Middle Eocene Exhumation of the Trans-Himalayan Ladakh Batholith, and the India–Asia Convergence. Curr. Sci. 113, 1090. https://doi.org/10.18520/cs/v113/i06/1090-1098.
Lakhan, N., Singh, A.K., Singh, B.P., Premi, K., Oinam, G., 2020a. Evolution of late cretaceous to Palaeogene basalt–andesite–dacite–rhyolite volcanic suites along the northern margin of the Ladakh magmatic arc, NW Himalaya. India. J. Earth Syst. Sci. 129, 108. https://doi.org/10.1007/s12040-020-1372-6.
Lakhan, N., Singh, A.K., Singh, B.P., Sen, K., Singh, M.R., Khogenkumar, S., Singhal, S., Oinam, G., 2020b. Zircon U–Pb geochronology, mineral and whole-rock geochemistry of the Khardung volcanics, Ladakh Himalaya, India: Implications for late cretaceous to Palaeogene continental arc magmatism. Geol. J. 55, 3297–3320. https://doi.org/10.1002/gj.3594.
Le Fort, P., 1989. The Himalayan Orogenic Segment, in: Şengör, A.M.C. (Ed.), Tectonic Evolution of the Tethyan Region. Springer Netherlands, Dordrecht, pp. 289–386. 10.1007/978-94-009-2253-2_16.
Leier, A.L., DeCelles, P.G., Kapp, P., Ding, L., 2007. The Takena Formation of the Lhasa terrane, southern Tibet: the record of a late cretaceous retroarc foreland basin. Geol. Soc. Am. Bull. 119, 31–48. https://doi.org/10.1130/B25974.1.
Long, S.P., Kohn, M.J., Kerswell, B.C., Starnes, J.K., Larson, K.P., Blackford, N.R., Soignard, E., 2020. Thermometry and Microstructural Analysis Imply Protracted Extensional Exhumation of the Tso Morari UHP Nappe, Northwestern Himalaya: Implications for Models of UHP Exhumation. Tectonics 39, e2020TC006482. https://doi.org/10.1029/2020TC006482.
Mahéo, G., Bertrand, H., Guillot, S., Villa, I.M., Keller, F., Capiez, P., 2004. The South Ladakh ophiolites (NW Himalaya, India): an intra-oceanic tholeiitic arc origin with implication for the closure of the Neo-Tethys. Chem. Geol. 203, 273–303. https://doi.org/10.1016/j.chemgeo.2003.10.007.
Martin, C.R., Jagoutz, O., Upadhyay, R., Royden, L.H., Eddy, M.P., Bailey, E., Nichols, C. I.O., Weiss, B.P., 2020. Paleocene latitude of the Kohistan–Ladakh arc indicates multistage India–Eurasia collision. Proc. Natl. Acad. Sci. 117, 29487–29494. https://doi.org/10.1073/pnas.2009039117.
Martin, C.R., Van Buer, N.J., Matchette-Downes, H., Mueller, P.A., Cruz-Uribe, A.M., Van Tongeren, J.A., Hanchar, J.M., Upadhyay, R., Jagoutz, O., 2025. The geology of the Shyok suture zone: evidence for cretaceous extension of the southern Eurasian margin and Eocene India–Eurasia collision. J. Geol. Soc. 182, jgs2024-082. https://doi.org/10.1144/jgs2024-082.
Mathur, N.S., Juyal, K.P., 1996. Time of emplacement of ophiolitic mélange in Indus Suture Zone. A palaeontological approach. Contrib. XV Indian Colloq. Micropaleontol. Stratigr, Ladakh Himalaya, pp. 169–176.
Mathur, N.S., Juyal, K.P., Kumar, K., 2009. Larger foraminiferal biostratigraphy of lower Paleogene successions of Zanskar Tethyan and Indus–Tsangpo Suture zones, Ladakh, India in the light of additional data. Himal. Geol. 30, 45–68.
Mathur, N.S., Juyal, K.P., Kumar, K., 2008. Biotic response to Cretaceous-Eocene tectonic events at the northern margin of the Indian Plate and the Indus-Tsangpo suture zone, Ladakh Himalaya. India. J. Palaeontol. Soc. India 53, 37–49. https://doi.org/10.1177/0971102320080105.
Mathur, N.S., Vogel, K., 1988. Some rudists from Khalsi limestone of Indus Formation, Ladakh Himalaya. Geobios 21, 693–707. https://doi.org/10.1016/S0016-6995(88)80088-3.
Mathur, Y.K., Jain, A.K., 1980. Palynology and age of the Dras volcanics near Shergol. Ladakh, Jammu and Kashmir, India.
Miller, C., Klötzli, U., Frank, W., Thöni, M., Grasemann, B., 2000. Proterozoic crustal evolution in the NW Himalaya (India) as recorded by circa 1.80 Ga mafic and 1.84 Ga granitic magmatism. Precambrian Res. 103, 191–206. https://doi.org/10.1016/S0301-9268(00)00091-7.
Murphy, M.A., Yin, A., Harrison, T.M., Dürr, S.B., Z, C., Ryerson, F.J., Kidd, W.S.F., X, W., X, Z., 1997. Did the Indo-Asian collision alone create the Tibetan plateau? Geology 25, 719. 10.1130/0091-7613(1997)025%253C0719:DTIACA%253E2.3.CO;2.
Najman, Y., Jenks, D., Godin, L., Boudagher-Fadel, M., Millar, I., Garzanti, E., Horstwood, M., Bracciali, L., 2017. The Tethyan Himalayan detrital record shows that India–Asia terminal collision occurred by 54 Ma in the Western Himalaya. Earth Planet. Sci. Lett. 459, 301–310. https://doi.org/10.1016/j.epsl.2016.11.036.
Ravikant, V., Wu, F.-Y., Ji, W.-Q., 2009. Zircon U–Pb and Hf isotopic constraints on petrogenesis of the Cretaceous–Tertiary granites in eastern Karakoram and Ladakh, India. Lithos 110, 153–166. https://doi.org/10.1016/j.lithos.2008.12.013.
Raz, U., Honegger, K., 1989. Magmatic and tectonic evolution of the Ladakh Block from field studies. Tectonophysics 161, 107–118. https://doi.org/10.1016/0040-1951(89)90306-5.
Reuber, I., 1989. The Dras arc: two successive volcanic events on eroded oceanic crust. Tectonophysics 161, 93–106. https://doi.org/10.1016/0040-1951(89)90305-3.
Reuber, I., 1986. Geometry of accretion and oceanic thrusting of the Spongtang Ophiolite, Ladakh-Himalaya. Nature 321, 592–596. https://doi.org/10.1038/321592a0.
Reuber, I., Colchen, M., Mevel, C., 1987. The geodynamic evolution of the South-Tethyan, margin in Zanskar, NW-Himalaya, as revealed by the Spongtang ophiolitic melanges. Geodin. Acta 1, 283–296. https://doi.org/10.1080/09853111.1987.11105146.
Reuber, I., Montigny, R., Thuizat, R., 1989. K-Ar ages of ophiolites and arc volcanics of the Indus suture zone : clues on the early evolution of the Neo-Tethys. Eclogae Geol. Helvetiae 82. https://doi.org/10.5169/SEALS-166398.
Reynolds, P.H., Brookfield, M.E., McNutt, R.H., 1983. The age and nature of Mesozoic-Tertiary magmatism across the Indus Suture Zone in Kashmir and Ladakh (N. W. India and Pakistan). Geol. Rundsch. 72, 981–1003. https://doi.org/10.1007/BF01848351.
Robertson, A., Degnan, P., 1994. The Dras arc complex: lithofacies and reconstruction of a late cretaceous oceanic volcanic arc in the Indus Suture Zone, Ladakh Himalaya. Sediment. Geol. 92, 117–145. https://doi.org/10.1016/0037-0738(94)90057-4.
Robertson, A.H.F., 2000. Formation of mélanges in the Indus Suture Zone, Ladakh Himalaya by successive subduction-related, collisional and post-collisional processes during late Mesozoic-late Tertiary time. Geol. Soc. Lond. Spec. Publ. 170, 333–374. https://doi.org/10.1144/GSL.SP.2000.170.01.19.
Robertson, A.H.F., Degnan, P.J., 1993. Sedimentology and tectonic implications of the Lamayuru complex: deep-water facies of the Indian passive margin, Indus Suture Zone, Ladakh Himalaya. Geol. Soc. Lond. Spec. Publ. 74, 299–321. https://doi.org/10.1144/GSL.SP.1993.074.01.21.
Rolland, Y., Picard, C., Pecher, A., Lapierre, H., Bosch, D., Keller, F., 2002. The cretaceous Ladakh arc of NW himalaya—slab melting and melt–mantle interaction during fast northward drift of Indian Plate. Chem. Geol. 182, 139–178. https://doi.org/10.1016/S0009-2541(01)00286-8.
Rowley, D.B., 1996. Age of initiation of collision between India and Asia: a review of stratigraphic data. Earth Planet. Sci. Lett. 145, 1–13. https://doi.org/10.1016/S0012-821X(96)00201-4.
Saktura, W.M., Buckman, S., Nutman, A.P., Bennett, V.C., 2021. Late Jurassic Changmar complex from the Shyok ophiolite, NW Himalaya: a prelude to the Ladakh Arc. Geol. Mag. 158, 239–260. https://doi.org/10.1017/S0016756820000400.
Schaltegger, U., Zeilinger, G., Frank, M., Burg, J., 2002. Multiple mantle sources during island arc magmatism: U–Pb and Hf isotopic evidence from the Kohistan arc complex, Pakistan. Terra Nova 14, 461–468. https://doi.org/10.1046/j.1365-3121.2002.00432.x.
Schärer, U., Xu, R.-H., Allègre, C.J., 1984. U-Pb geochronology of Gangdese (Transhimalaya) plutonism in the Lhasa-Xigaze region. Tibet. Earth Planet. Sci. Lett. 69, 311–320. https://doi.org/10.1016/0012-821X(84)90190-0.
Schlup, M., Carter, A., Cosca, M., Steck, A., 2003. Exhumation history of eastern Ladakh revealed by ^{40} Ar/^{39} Ar and fission-track ages: the Indus River–Tso Morari transect, NW Himalaya. J. Geol. Soc. 160, 385–399. https://doi.org/10.1144/0016-764902-084.
Searle, M., Corfield, R.I., Stephenson, B., Mccarron, J., 1997. Structure of the North Indian continental margin in the Ladakh–Zanskar Himalayas: implications for the timing of obduction of the Spontang ophiolite, India–Asia collision and deformation events in the Himalaya. Geol. Mag. 134, 297–316. https://doi.org/10.1017/S0016756897006857.
Searle, M.P., Pickering, K.T., Cooper, D.J.W., 1990. Restoration and evolution of the intermontane Indus molasse basin, Ladakh Himalaya, India. Tectonophysics 174, 301–314. https://doi.org/10.1016/0040-1951(90)90327-5.
Searle, M.P., Windley, B.F., Coward, M.P., Cooper, D.J.W., Rex, A.J., Rex, D., Tingdong, L., Xuchang, X., Jan, M.Q., Thakur, V.C., Kumar, S., 1987. The closing of Tethys and the tectonics of the Himalaya. GSA Bull. 98, 678–701. https://doi.org/10.1130/0016-7606(1987)98%253C678:TCOTAT%253E2.0.CO;2.
Sharma, K., Sinha, A.K., Baydasarian, G., Gukasien, R., 1978. K/Ar dating of the Dras Volcanics, Shyok Volcanics and the Ladakh Granite, Ladakh, Northwest Himalaya. Himal. Geol. 8, 288–295.
Sharman, G.R., Malkowski, M.A., 2020. Needles in a haystack: Detrital zircon U Pb ages and the maximum depositional age of modern global sediment. Earth-Sci. Rev. 203, 103109. https://doi.org/10.1016/j.earscirev.2020.103109.
Shellnutt, J.G., Lee, T.-Y., Brookfield, M.E., Chung, S.-L., 2014. Correlation between magmatism of the Ladakh Batholith and plate convergence rates during the India–Eurasia collision. Gondwana Res. 26, 1051–1059. https://doi.org/10.1016/j.gr.2013.09.006.
Sinclair, H.D., Jaffey, N., 2001. Sedimentology of the Indus Group, Ladakh, northern India: implications for the timing of initiation of the palaeo-Indus River. J. Geol. Soc. 158, 151–162. https://doi.org/10.1144/jgs.158.1.151.
Singh, N.L., Akhtar, S., Singh, A.K., Singh, B.P., Saikia, A., Jeelani, S.H., 2023. Petrogenesis and tectonic implications of the late cretaceous to Paleogene calc-alkaline volcanic rocks. Ladakh Himalaya. J. Asian Earth Sci. 253, 105700. https://doi.org/10.1016/j.jseaes.2023.105700.
Sinha, A.K., Upadhyay, R., 1993. Mesozoic neo-tethyan pre-orogenic deep marine sediments along the Indus-Yarlung Suture, Himalaya. Terra Nova 5, 271–281. https://doi.org/10.1111/j.1365-3121.1993.tb00258.x.
Steck, A., 2003. Geology of the NW Indian Himalaya. Eclogae Geol. Helvetiae 96, 147–196. https://doi.org/10.5169/SEALS-169014.
Sterne, E.J., 1979. Report on geological traverses across the Indus-Tsangpo suture zone in Ladakh, northern India.
Sutre, E., 1990. Les formations de la marge néotethysienne et les mélanges ophiolitiques de la zone de suture de l'Indus en Himalaya du Ladakh - Inde. - Stratigraphie, tectonique, évolution géodynamique. Université de Poitiers, Poitiers.

Taylor, S.R., McLennan, S.M., 1985. The continental crust: its composition and evolution. Blackwell Scientific Pub, Palo Alto, CA, United States.

Tewari, B.S., Pande, I.C., Kumar, R., 1970. Lower cretaceous fossiliferous limestone from Khalsi. Ladakh. Cent. Adv. Study Geol. 7, 197–200.

Thakur, V.C., Virdi, N.S., 1979. Lithostratigraphy, structural framework, deformation and metamorphism of the Southeastern region of Ladakh, Kashmir Himalaya. India. Himal. Geol. 9, 63–78.

Tripathy-Lang, A., Hodges, K.V., Van Soest, M.C., Ahmad, T., 2013. Evidence of pre-Oligocene emergence of the Indian passive margin and the timing of collision initiation between India and Eurasia. Lithosphere 5, 501–506. https://doi.org/10.1130/L273.1.

Upadhyay, R., Ram-Awatar, Kar, R.K., Sinha, A.K., 2004. Palynological evidence for the Palaeocene evolution of the forearc basin, Indus Suture Zone, Ladakh, India. Terra Nova 16, 216–225. 10.1111/j.1365-3121.2004.00553.x.

Upadhyay, R., Sinha, A.K., 1998. Tectonic evolution of Himalayan Tethys and subsequent Indian plate subduction along Indus Suture Zone. Proc. Indian Natl. Sci. Acad. 64, 659–683.

Van Haver, T., 1984. Etude stratigraphique, sédimentologique et structurale d'un bassin d'avant arc: exemple du bassin de l'Indus, Ladakh. Université Scientifique et Médicale de Grenoble. Himalaya (Doctoral dissertation.

Vermeesch, P., 2021. On the treatment of discordant detrital zircon U–Pb data. Geochronology 3, 247–257. https://doi.org/10.5194/gchron-3-247-2021.

Villalobos-Orchard, J., Debret, B., Bouilhol, P., Upadhyay, R., Gutiérrez, P., Chauvel, C., Girault, F., 2025. Geochemical signatures of forearc serpentinites from oceanic to continental subduction. Geochim. Cosmochim. Acta 392, 1–16. https://doi.org/10.1016/j.gca.2024.11.001.

Walsh, J.M.J., Buckman, S., Nutman, A.P., Zhou, R., 2021. The significance of Upper Jurassic felsic volcanic rocks within the incipient, intraoceanic Dras Arc, Ladakh. NW Himalaya. Gondwana Res. 90, 199–219. https://doi.org/10.1016/j.gr.2020.11.007.

Walsh, J.M.J., Buckman, S., Nutman, A.P., Zhou, R., 2019. Age and Provenance of the Nindam Formation, Ladakh, NW Himalaya: Evolution of the Intraoceanic Dras Arc before Collision with India. Tectonics 38, 3070–3096. https://doi.org/10.1029/2019TC005494.

Wang, C., Ding, L., Xiong, Z., Allen, M.B., Laskowski, A.K., Garzanti, E., Zhang, Q., Cai, F., Wang, H., Song, P., Li, Y., Ping, F., Farnsworth, A., Lunt, D.J., Valdes, P.J., Li, Z., Wu, C., Qasim, M., 2025. Timing of initial collision and suturing processes in the Himalaya and Zagros. Nat. Rev. Earth Environ. 6, 357–376. https://doi.org/10.1038/s43017-025-00669-8.

Wen, D., Liu, D., Chung, S., Chu, M., Ji, J., Zhang, Q., Song, B., Lee, T., Yeh, M., Lo, C., 2008. Zircon SHRIMP U–Pb ages of the Gangdese Batholith and implications for Neotethyan subduction in southern Tibet. Chem. Geol. 252, 191–201. https://doi.org/10.1016/j.chemgeo.2008.03.003.

Wu, F.-Y., Clift, P.D., Yang, J.-H., 2007. Zircon Hf isotopic constraints on the sources of the Indus Molasse, Ladakh Himalaya, India. Tectonics 26, n/a-n/a. https://doi.org/10.1029/2006TC002051.

Xu, R.-H., Schärer, U., Allègre, C.J., 1985. Magmatism and Metamorphism in the Lhasa Block (Tibet): a Geochronological Study. J. Geol. 93, 41–57. https://doi.org/10.1086/628918.

Zhang, Z., An, W., Palin, R.M., Ding, H., Dong, X., Tian, Z., 2023. Intraoceanic Subduction System within the Neo-Tethys: evidence from late cretaceous Arc Magmatic Rocks of the Eastern Himalaya. Geochem. Geophys. Geosystems 24, e2023GC011214. https://doi.org/10.1029/2023GC011214.

Zhou, R., Aitchison, J.C., Lokho, K., Sobel, E.R., Feng, Y., Zhao, J., 2020. Unroofing the Ladakh Batholith: constraints from autochthonous molasse of the Indus Basin, NW Himalaya. J. Geol. Soc. 177, 818–825. https://doi.org/10.1144/jgs2019-188.

Zyabrev, S.V., Kojima, S., Ahmad, T., 2008. Radiolarian biostratigraphic constraints on the generation of the Nidar ophiolite and the onset of Dras arc volcanism: Tracing the evolution of the closing Tethys along the Indus – Yarlung-Tsangpo suture. Stratigraphy 5, 99–112. https://doi.org/10.29041/strat.05.1.07.